SAND75-0278
Unlimited Release

Solar Total Energy Program Semiannual Report October 1974 – March 1975

Solar Energy Projects Division 5712
Solar Energy Systems Division 5717

Prepared by Sandia Laboratories, Albuquerque New Mexico 87115 and Livermore, California 94550 for the United States Energy Research and Development Administration under Contract AT (29-1) 789
Printed July 1975

Sandia Laboratories
energy report

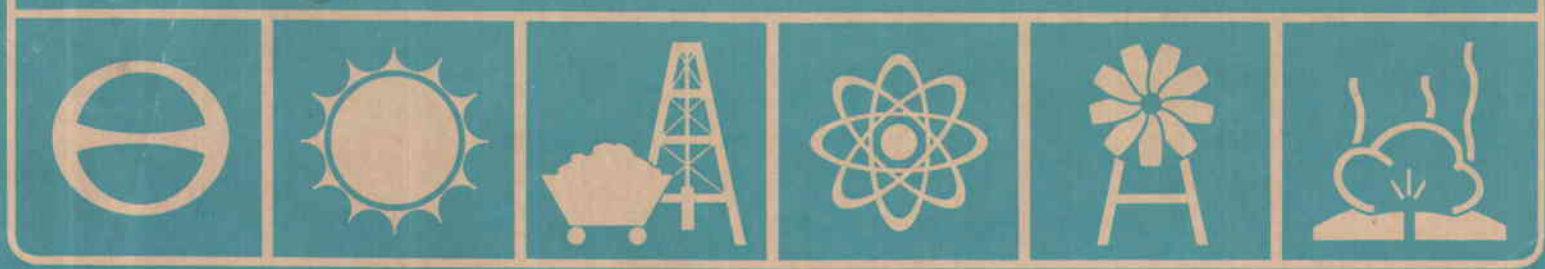

Issued by Sandia Laboratories, operated for the United States Energy Research and Development Administration by Sandia Corporation.

SAND75-0278
Unlimited Release
Printed July 1975

SOLAR TOTAL ENERGY PROGRAM SEMIANNUAL REPORT
October 1974 - March 1975

Edited by R. W. Harrigan
Solar Energy Systems Division, 5717
Sandia Laboratories, Albuquerque, NM 87115

ABSTRACT

This report describes the activities of the Sandia Laboratories Solar Total Energy Program during the 6-month period, October 1974 through March 1975. Included are highlights of the period, descriptions of the system and its components, including recent modifications, and the results of systems analyses and component testing.

Printed in the United States of America

Available from
National Technical Information Service
U. S. Department of Commerce
5285 Port Royal Road
Springfield, Virginia 22151
Price: Printed Copy $5.45; Microfiche $2.25

CONTENTS

CONTENTS (cont.)

LIST OF TABLES

FIGURES

SOLAR TOTAL ENERGY PROGRAM SEMIANNUAL REPORT
October 1974 - March 1975

SECTION I. INTRODUCTION

The Solar Total Energy Program is the outgrowth of a series of exploratory system studies conducted at Sandia Laboratories since 1972, concerning potential uses of solar energy.

The studies have coalesced into the concept of a cascaded system in which solar energy collected at a central area is used to provide electrical power, heating, air-conditioning, and hot water to a wide spectrum of users. A comprehensive hardware program designed to demonstrate one solar total energy concept is being conducted concurrently with systems analyses performed to investigate various additional means of implementing solar total energy concepts.

The primary objective of the Solar Total Energy Program is to determine and demonstrate the technical and economic feasibility of solar total energy systems for a variety of sites and loads. Additional objectives of the overall program are (1) to encourage private sector participation in the program and in the development of components for the system, (2) to determine those areas of research and development that offer the greatest payoffs, (3) to develop and validate a systems analysis computer program capable of evaluating the great number of possible combinations of total energy system configurations, and (4) to provide a system (Solar Total Energy Test Facility), prior to the pilot plant stage, sufficiently versatile to be used as an engineering evaluation center for further development of individual components or other solar energy subsystems.

This report marks the initiation of semiannual reporting periods and has seen the transition of all funding for the program from the National Science Foundation and the Atomic Energy Commission to the Energy Research and Development Administration. Within this program, work is also being conducted to extend systems analyses to a widespread range of potential applications and systems concepts. The progress of this work will also be reported herein.

The Solar Total Energy System, depicted in block diagram form in Figure 1 and as an artist's concept in Figure 2, will operate as follows. A working fluid is heated in the receiver tubes of the solar collectors by reflected and focused solar radiation. This fluid is pumped to the high-temperature storage tank. On a demand basis, fluid is extracted from this storage to the toluene boiler which produces superheated vapor to power the turbine/generator. The boiler can also be operated from a fossil-fuel-fired heater to insure continuity of operation during extended cloudy periods. Turbine condenser coolant collected in the low-temperature fluid storage tank becomes

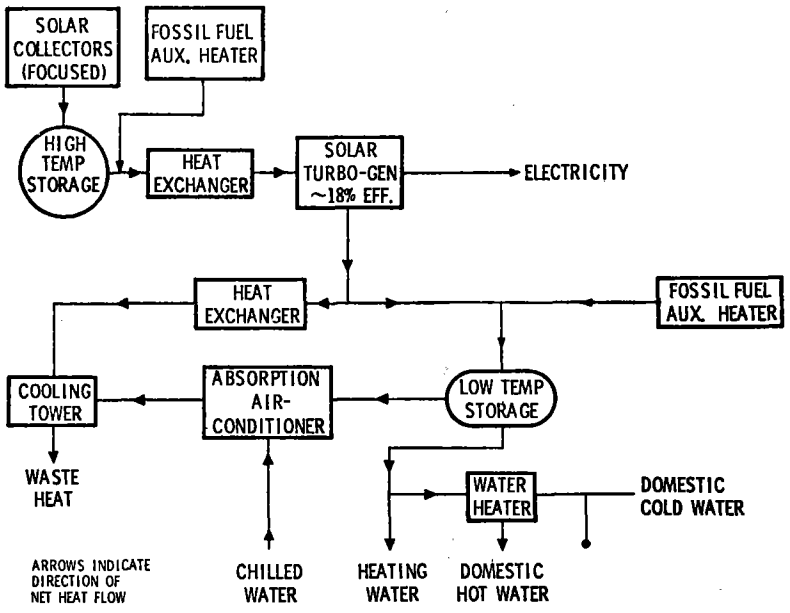

Figure 1. Solar Total Energy System Simplified Schematic

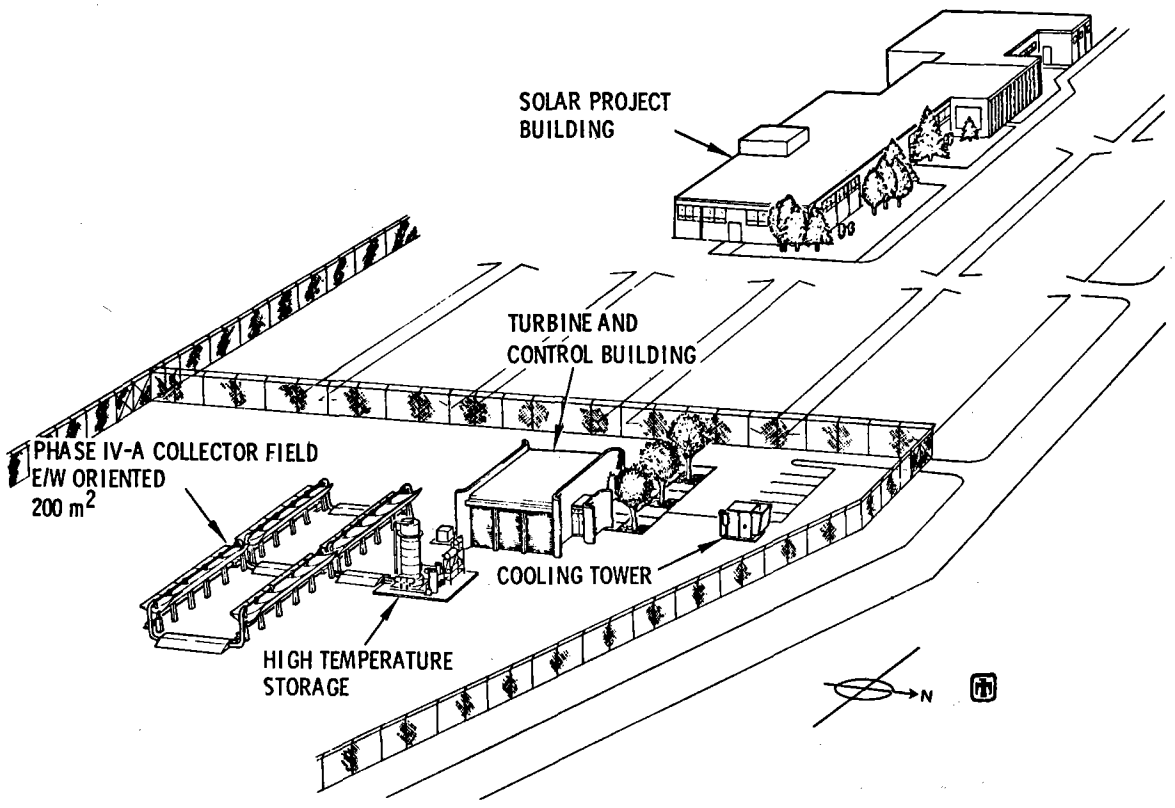

Figure 2. Solar Total Energy Test Facility

the energy source for the low-temperature portion of the system. On a demand basis, fluid is extracted from low-temperature storage to power heating, air-conditioning, and hot-water-heating components.

The overall Solar Total Energy Program consists of seven phases of which the work being reported in this document is the beginning of Phase IV. The program, which was initiated in 1972 with background research and exploratory analysis, has progressed to the present hardware stage in which the test bed Solar Total Energy System is being built to provide power for an 1100 m^2 office building, the Solar Project Building. The program will conclude with the construction and operation of a solar total energy pilot plant expected to be achieved in cooperation with commercial interests.

Phases I, II, and III, which have emphasized preliminary studies and designs, have been completed. Phase IV-A began in July 1974. Phase IV-A is the pivotal phase in that it marks the transition from the analysis and design effort to the hardware and construction effort. Approximately 25 percent of the high-temperature solar-to-electric portion of the system is to be put into operation during this phase. Data collection in the high-temperature regime is of primary importance because little operating experience in this area has been accumulated.

During Phase IV-B, the remainder of the solar-to-electric components will be added, and the cascaded low-temperature portion of the system (heating, air-conditioning, and hot water) will be installed.

Phase V will consist of operating the test bed under various conditions to gather and analyze engineering data which can provide a basis for the design of the pilot plant and for future solar energy systems. During this phase, the feasibility of powering and heating the Solar Project Building will be demonstrated.

Phases VI and VII will consist of the design, construction, and operation of a pilot commercial solar power plant. The overall Solar Total Energy Program plan and major milestones are illustrated in Figure 3.

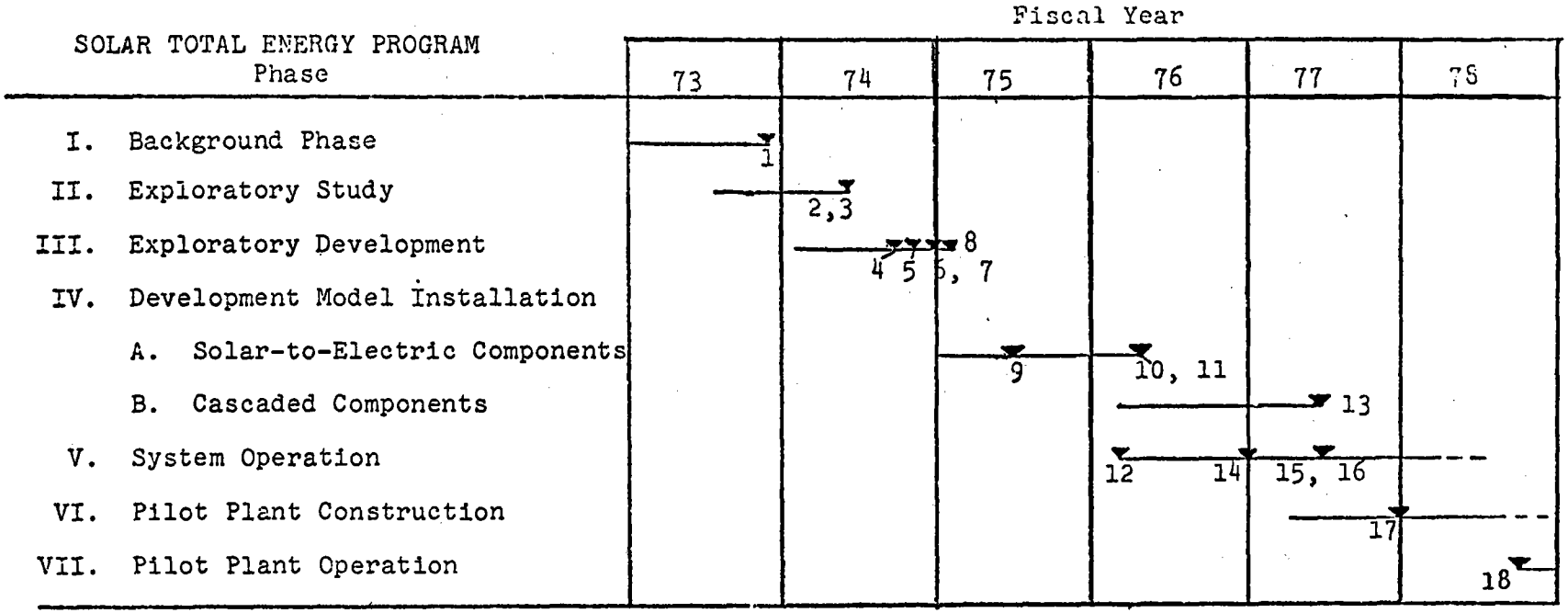

Milestones:

1. Completion of Phase I
2. Preliminary system design complete
3. Economic evaluation complete
4. Collector evaluation facility complete
5. System analysis program operational
6. Baseline system design complete
7. Phase IV-A proposal submitted
8. Phase IV-A supplementary proposal submitted
9. System analysis program loads profiles established
10. Partial collector field, storage, and turbine-generator test bed complete
11. Solar and weather input data established
12. Initial operation of partial Solar Total Energy test bed
13. Remainder of Solar Total Energy System completed
14. System analysis program refined and revalidated
15. Operation of complete Solar Total Energy System
16. Demonstration of Solar Project Building
17. Pilot plant designed
18. Pilot plant operational

Figure 3. Solar Total Energy Program Schedule and Milestones

SECTION II. OVERVIEW OF ACTIVITIES

Highlights

The following activities and milestones highlighted this reporting period:

- Solar collector field and turbine/control building construction started.
- Contract for portion of Phase IV-A of program approved by NSF.
- Program responsibility transferred to ERDA.
- Final phase (construction) of turbine/generator contract initiated.
- Two 9 x 12 foot, north-south, tilted collectors installed at collector test facility.
- Tracking and drive system testing initiated.
- Phase IV-A system design frozen.
- Orders placed for all major hardware items.
- Transient collector/fluid loop model operational.
- Testing of collector receiver tube parameters in progress.
- Systems analysis of several total energy systems initiated.
- Completion of analysis of 1000-separate-homes community.
- Identification of a flexible mixed-load community.
- Storage test facility completed and testing initiated on total energy system storage tank.
- Full-scale prototype 9 x 12 foot, east-west reflectors received.
- Selective black surface established for Phase IV-A receivers (α = 0.95, ϵ = 0.21 at 600°F; black chrome).
- Basic control strategy for all fluid loops established.
- Decision made to adopt vapor-deposited metal on Teflon and Mylar for reflector surfaces.
- Contract initiated with turbine supplier for Rankine cycle dynamic response model specific to solar power operation.
- Storage-to-turbine fluid loop transient control model initiated.

Reports and Presentations

The following reports and presentations have been completed in support of the Solar Total Energy Program during the reporting period.

Reports

1. J. P. Abbin and W. R. Leuenberger, "Program CYCLE: A Rankine Cycle Analysis Routine," SAND74-0099, Sandia Laboratories, October 1974.

2. J. A. Leonard and S. Thunborg, "Solar Total Energy Program Quarterly Report, July-September 1974," SAND74-0391, Sandia Laboratories, December 1974.

3. G. V. Barton, "A Preliminary Analysis of Combined Solar Photovoltaic-Thermal Systems for Terrestrial Applications," SAND74-0398, Sandia Laboratories, January 1975.

Presentations

1. R. P. Stromberg, "Sandia Laboratories Solar Total Energy Program," New Mexico Solar Energy Association, Ghost Ranch, New Mexico, October 13, 1974.

2. J. P. Abbin, "Cycle - A Computer Program to Model and Analyze Rankine Cycle Systems," Lawrence Livermore Laboratory Meeting on Computer Use by Engineers, Livermore, California, October 23-25, 1974.

3. J. Cyrus, "Solar Total Energy System," University of New Mexico, Mechanical Engineering Department, Albuquerque, New Mexico, November 2, 1974.

4. B. W. Marshall, "Solar Energy Research at Sandia Laboratories," ASME Student Chapter, Texas Tech, Lubbock, Texas, November 7, 1974.

5. R. W. Harrigan, "Solar Energy Utilization," Environmental Improvement Agency of New Mexico, Albuquerque, New Mexico, November 9, 1974.

6. R. P. Stromberg, "Solar Energy and the Sandia Solar Total Energy Program," AIME, Carlsbad Potash Section, Carlsbad, New Mexico, November 19, 1974.

7. M. W. Edenburn, "Sandia Laboratories' Solar Energy System Simulation Program," Department of Mechanical Engineering, University of New Mexico, Albuquerque, New Mexico, November 25, 1974.

8. R. P. Stromberg, "Solar Energy Research," Harvard-Yale-Princeton Club, Albuquerque, New Mexico, December 2, 1974.

9. M. W. Edenburn, B. W. Marshall, and R. P. Stromberg, "Sandia's Solar Energy System Analysis Project," National Science Foundation, American Gas Association, Atomic Energy Commission, Washington, D. C., December 10-11, 1974.

10. R. P. Stromberg, "Solar Energy Television Program," New Mexico Cable Television, Santa Fe, New Mexico, January 6, 1975, Participants: Ed Kist, Public Service Company of New Mexico; Steve Baer, Zomeworks; and Keith Haggard, New Mexico Solar Energy Association.

11. R. W. Harrigan, "Sandia Solar Total Energy Systems Analysis," Mechanical Engineering Department, SCORE Competition Group, The University of New Mexico, Albuquerque, New Mexico, January 7, 1975.

12. R. P. Stromberg, "Solar Energy," Rio Grande High School, Albuquerque, New Mexico, January 7, 1975.

13. R. H. Braasch, "Sandia Total Energy Program Review," Mechanical Engineering Department, SCORE Competition, The University of New Mexico, January 13, 1975.

14. R. P. Stromberg, "Solar Total Energy," American Bar Foundation, Washington, D. C., February 10, 1975.

15. R. P. Stromberg, "Sandia Solar Total Energy Program," American Gas Association Marketing Group, San Diego, California, February 13, 1975.

16. R. P. Stromberg, "Solar Total Energy System," Engineers Day, Western Electric, Hawthorne Plant, Chicago, Illinois, February 18, 1975.

17. B. W. Marshall, "Solar Energy Activities at Sandia Laboratories," Los Altos Kiwanis Club, Albuquerque, New Mexico, February 20, 1975.

18. R. P. Stromberg, R. H. Braasch, and J. A. Leonard, "Solar Total Energy Program Review," ERDA, Washington, D. C., February 25, 1975.

19. R. P. Stromberg, "Solar Energy," American Training Association Meeting, Albuquerque, New Mexico, March 6, 1975.

20. R. W. Harrigan, "Solar Energy," Valley High School ROTC, Albuquerque, New Mexico, March 7, 1975.

21. E. C. Boes, "Estimation of Direct Normal Radiation," Terrestial Photovoltaics Measurements Workshop, NASA-Lewis, Cleveland, Ohio, March 19-21, 1975.

SECTION III. SYSTEM DESCRIPTION AND STATUS

Phase IV of the Solar Total Energy Program has been organized into a work breakdown structure of tasks and subtasks. This section presents the detailed status of each program task.

Task 1. Program Management

The work breakdown structure was expanded during this reporting period to more fully delineate the Fluid Transfer system tasks. Task 4 was expanded to include the Storage Fluid Transfer System. Tasks 5.7 and 5.8 were added to include the Condenser Fluid Transfer System and the Cooling Tower Fluid Transfer System. These tasks were previously included as parts of other tasks and their addition does not represent an increase in the work to be performed. The complete breakdown of work into tasks is given in the Contents (page 5). A chart illustrating program management structure is shown in Appendix B.

Task 2. System Management

2.1 System Engineering

Recent performance predictions of the turbine Rankine cycle system indicate cycle efficiencies and storage ΔT's lower than previous predictions, attributed to parasitic losses from subcomponents and to larger than anticipated temperature and pressure drop from the vapor generator to the turbine. As a result, the fluid flow and heat transfer rates have changed throughout the system. Figure 4 is a revised version of the system schematics and reflects the effects of these changes; for a further discussion, see Section 5.2. The overall effect is to increase required collector area by 16% as a result of less cycle efficiency and to increase storage volume by 23% as a result both of decreased storage ΔT and less cycle efficiency.

Sizing of Collectors for Phase IV-B -- A study has been undertaken to determine optimum collector size using the approach described in a recent publication.* For a given liquid flow rate, smaller receiver tubes, resulting in higher liquid film coefficients, transfer the solar energy incident on the tube to the liquid within more effectively. Also heat losses from the receiver tube decrease as the tube diameter decreases. Smaller receiver tube diameters result in smaller reflection widths since the farthest reflector-to-tube distance determines the receiver tube diameter.† While smaller receiver tubes would appear desirable for improved energy collection, the

*G. W. Treadwell, "Selection of Parabolic Solar Collector Field Arrays," SAND74-0375, Sandia Laboratories, May 1975.

†G. W. Treadwell and W. H. McCulloch, "Design Analysis of Asymmetric Solar Receivers," SAND74-0124, Sandia Laboratories, August 1974.

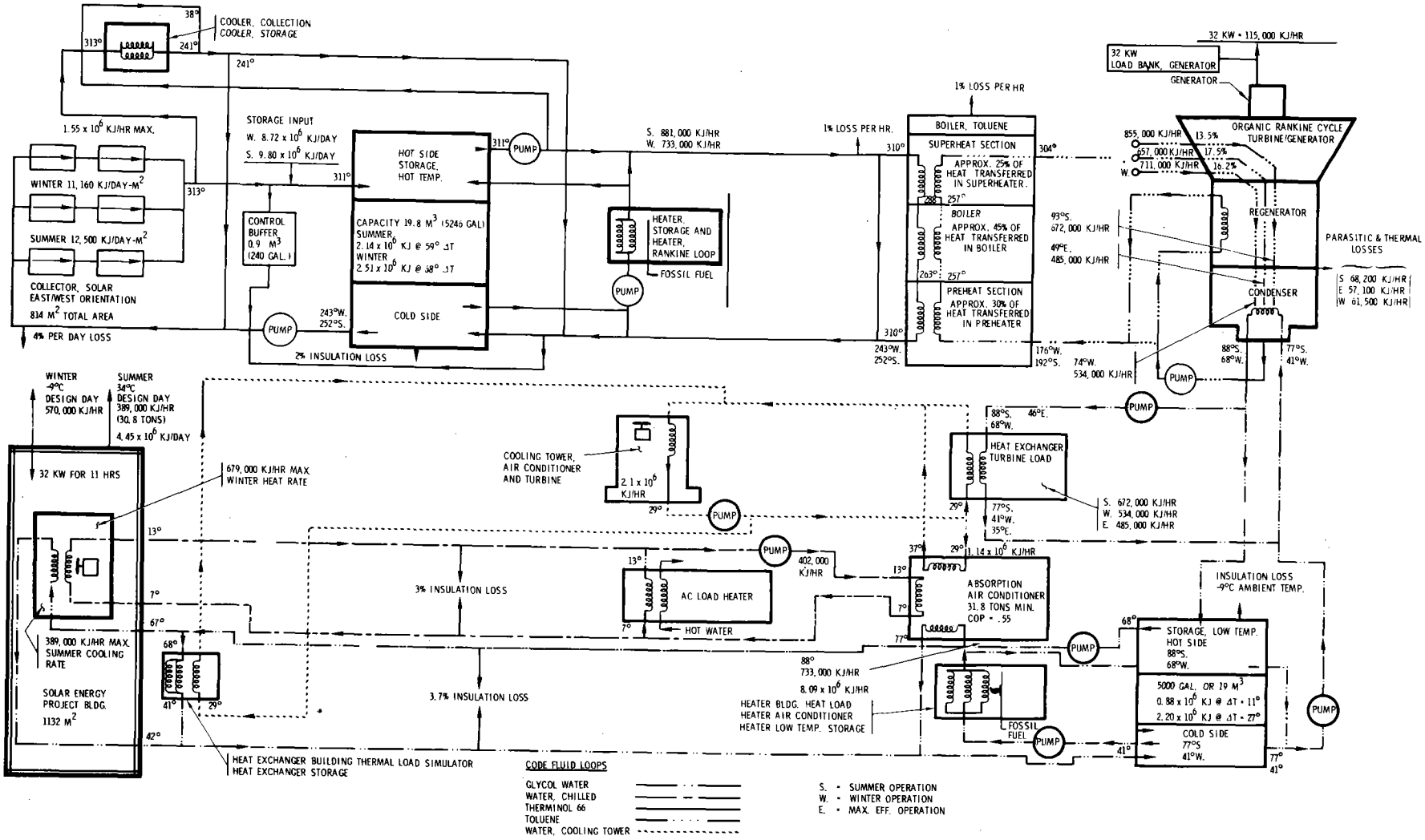

Figure 4. Solar Total Energy System Schematic

resulting higher fluid friction losses provide practical limits to size reduction. For example, if a maximum of 1% of the collected energy may be devoted to offsetting friction losses in the receiver tube, the limit of receiver tube size is determined to be 2.868 cm (1.25 in.). This in turn defines a collector width of 1.83 m (6 ft).

The 2.74 x 3.66 m (9 x 12 ft) collector size for Phase IV-A was chosen as the largest conveniently handled by a commercial contractor and because that length is a multiple of readily available Alzac (Alcoa's lighting sheet reflector) sheet widths. (Shipping considerations were also a factor; much larger sizes would make transportation of an integral collector difficult.) Subsequently, reflector materials not size limited and potentially superior to Alzac have become available, thus precipitating the size-optimization study.

A computer study was conducted in which two collector sizes, A and B, were compared: A is 2.74 x 3.66 m (9 x 12 ft), B is 1.83 x 5.49 m (6 x 18 ft). For flow rates resulting in a ΔT/collector of 10°C, the results are summarized as follows:

1. B is more efficient than A when no turbulence generator is used.
2. A must have a turbulence generator to prevent liquid overheating (or the allowable temperature rise per collector must be decreased significantly).
3. The use of evacuated annuli and insulator strips causes minimal efficiency differences between the A and B collectors whether or not turbulence generators are used.
4. B can operate at temperatures closer than A to the liquid decay temperatures.
5. A has lower friction losses than B for the same volume flow rate and can operate over a greater span of flow rates without excessive pumping work.

B should be less expensive to construct because of its shorter span and reduced wind loading. The studies will continue for flow rates resulting in lower ΔT/collector. Lower ΔT/collector will require greater flow rates and, in general, will cause an advantage for B due to lower friction losses. The goal of these studies is to determine the reflector size for the collectors to be fabricated in Phase IV-B.

2.2 Systems Analysis

Program SOLSYS -- The Solar Energy Systems Simulation Program, SOLSYS, has been outlined in previous progress reports. (A comprehensive description of the program has been published.*) During the current report period, the following subroutines have been added to SOLSYS:

1. HALFDEM, a component which receives a fluid flow from its upstream component, divides the flow and sends it through two outlets. The flow rate sent through the first outlet is determined by the demand from a downstream component. The flow

* M. W. Edenburn and N. R. Grandjean, "Energy System Simulation Computer Program - SOLSYS," SAND75-0048, Sandia Laboratories, June, 1975

rate sent through the second outlet is the difference between the inlet flow rate and the first outlet flow rate.

2. WEATH8 reads hourly weather data from a magnetic tape. The weather data consists of the following:

   a. Wind direction (degrees from north)
   b. Wind speed (m/s)
   c. Dry bulb temperature (K)
   d. Wet bulb temperature (K)
   e. Dew point (K)
   f. Relative humidity (percent)
   g. Atmospheric pressure (N/m^2)
   h. Fractional opaque sky cover

   The data were taken from 1962-63 National Climatic Center records for the following eight locations:

City	Station No.
Albuquerque	23050
Boston	14739
Fort Worth	03927
Los Angeles	23174
Miami	12839
Nashville	13897
Omaha	14942
Seattle	24233

3. SOLEN3 provides solar data input for SOLSYS. The data consist of four weeks of actual recordings of the intensities for both direct normal incident radiation and total radiation on a horizontal surface. The four weeks of data were selected as described in 8.2 to provide samples of solar data which are representative of the four seasons in Albuquerque.

4. ELECTRQ provides electrical load data from two hourly data tables read as input. Schedule 1 is the primary load schedule and Schedule 2 is used for a specified number of days at weekly intervals, e.g., weekends. During specified shutdown periods no electricity is required.

Solar Total Energy Test Facility Simulation -- The basic objectives of the test facility are (1) provide a test system for evaluating system performance subject to various types of loads, (2) provide a test system for evaluating individual components, and (3) provide a building (Sandia Laboratories' Bldg. 832) with electricity, heating, and air conditioning. Analyses using SOLSYS have been conducted to determine test facility requirements (collector array size, storage size,

etc.) for a load comprising a small neighborhood of single family homes in support of objective 1, and to determine system design requirements for providing the energy needs for Bldg. 832 in support of objective 3. Performing the systems analysis for objective 3 will enable a comparison with actual performance, thus lending a degree of reality to the simulation.

The requirements for the Bldg. 832 system is compared to the planned test facility in Table I. It can be seen that the collector field and storage units will accommodate the loads of Bldg. 832. Computed collector field pumping powers are less than 1 kW for both north-south and east-west collector fields, which is in agreement with the test bed pump sizes. Collector field heat losses from the piping system are 10% and 2.5% of collected energy for the north-south and east-west collector systems, respectively. This demonstrates that the pipe insulation thicknesses planned for the test facility are not unreasonable. The low temperature loop cooling tower must be capable of dissipating 2×10^5 J/s (6.8×10^5 Btu/hr) which is within the capabilities of the tower planned. Parameters for the planned test bed system and for the Bldg. 832 system are in close agreement with the exception of the low temperature storage unit which is purposely oversized to provide future flexibility.

TABLE I

Sandia Laboratories Solar Energy Test Facility Applications

(E-W oriented collectors)

	Planned Test Bed	Bldg. 832	18 Houses	17 Houses	10 Houses	1 House
Peak Electric Load (kW)	32	32	32	30	18	2
Collector Array (m^2)	702	676	729	689	405	41
High-Temperature Storage (m^3)	16	13	28	26	16	2
Low-Temperature Storage (m^3)	19	7	74	70	41	4

The test facility is also intended to be used for studying system performance when applied to various other loads. Simulating an 18-home load (Table I) would require additional collectors and storage, simulating 17 homes would require additional high- and low-temperature storage, and 10 homes would require additional low-temperature storage only.

Table II compares the primary fuel (fossil fuel for electric generation and thermal needs) which would be used by a conventional, nontotal energy system with the computation of fuel needed as backup in the solar total energy system for Bldg. 832. Clear day fuel savings are significant; however, cloudy weather will reduce fuel savings.

TABLE II

Fossil Fuel Energy Used by Bldg. 832 With
Standard and Solar Energy Sources

(All Units J x 10^9/day)

	Winter	Spring	Summer
Standard System			
Electricity (30% conversion efficiency)	4.23	4.23	4.23
Heating (80% conversion efficiency)	8.91	3.78	0
Air conditioning (0.55 (COP)	0	0	3.18
TOTAL	13.14	8.01	7.41
Solar System			
Auxiliary Fuel (clear day)	1.08	0	0

Economic Analysis -- The previous quarterly report described the computer subroutines written to perform economic comparisons. A series of sample calculations were included, illustrating the level annual revenue requirements for single homes, based on a set of assumed future energy prices. These calculations have been extended to include comparison with solar total energy systems.

Fuel Costs -- The NSF Phase 0 studies for heating and cooling of buildings* included predictions of future energy costs. Local supply situations heavily influence anticipated rate changes (Figure 5), making it impossible to establish a consensus concerning future fuel prices for the U.S. in general.

Eight cities (see Task 8.2), representing a good cross section of the various types of weather conditions found in the U.S., have been chosen from the results of the NSF Phase 0 study. Utilities and other fuel suppliers in these locations have been contacted for their best estimate of future energy prices. These estimates have reflected the variations reported in the NSF Phase 0 study; one region suffering gas shortages may be converting to oil while another may expect coal to most strongly influence future fuel prices. Thus, it appears desirable to estimate future trends separately for each location.

Future prices for natural gas energy in the Albuquerque area were estimated, after consultation with local utility personnel, and used for the first set of comparisons. These are as follows:

	$/MBtu		
	Source	City Gate	Residence
Today	0.30	0.45	1.10
Near Future	0.80	1.00	1.80
1985	2.00	2.50	3.50
2020	3.00	3.75	5.50

*NSF-RA-N-74-021A (General Electric), -022A (TRW), and -023A (Westinghouse).

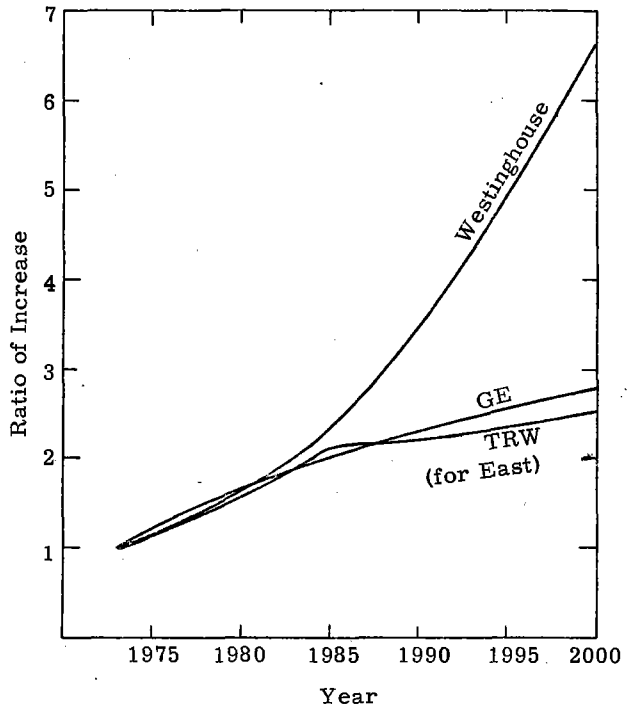

Figure 5. Ratio of Increase of Residential Gas Prices From 1973 Price (constant dollars)

As other locations are studied, additional estimates will be constructed.

Systems Costs -- For purposes of economic analysis, the solar total energy power plant is divided into five general categories: power generation plant, transmission plant, electric distribution plant (No. 1), thermal distribution plant (No. 2), and a general plant. For each of these costs are counted in two classifications: initial investment and future costs. Initial investments include land and land rights costs, buildings and improvements, and equipment costs. Salvage value of the equipment is also included. Future costs include operating, maintenance, and fuel costs--also major replacement and overhead costs which may be chosen at a rate and schedule to reflect the anticipated performance and operation of the different pieces of equipment.

The power generation plant includes the cost of solar collectors, storage, turbine systems, and the other components necessary to convert solar energy to electrical and thermal energy. The transmission plant includes costs of the equipment necessary to transmit electrical energy from the plant to the start of the distribution system. Distribution plant No. 2 is the thermal distribution system required to deliver the thermal energy to the users; distribution plant No. 1 represents the distribution network required to deliver electrical energy; and the general plant includes that portion of the plant required for management personnel, accounting, customer relations, etc. An example of the costs used in the analysis of a particular solar total energy system is given in the Appendix.

Economic Factors Excluding Fuel -- In the calculation of level annual revenue requirements for both solar and fossil-fueled energy systems, several economic factors must be considered. Future prices of goods and services are affected by the inflation rate. Cost of financing is affected by the long-term interest rate on money. Financing for a solar energy system serving a number of buildings in a community will be affected by the stock dividend rate required to secure risk capital.

Past data are available on all economic factors while future predictions are difficult to obtain. The Consumer Price Index has increased an average of 2.6% per year for the last 20 years, but in the last few years has shown a dramatic increase. Since future rates are difficult to estimate, a parametric study encompassing several rates was performed. Conversations with local utility rate personnel established the following values:

Inflation Rate	Cost of Money	Stock Dividend Rate
7.5	10.9	10.0
5.0	8.4	8.5
3.5	6.0	8.0
2.6	6.0	8.0

Inflation rates cited cover a range from the past 20-year average to near current rates. The cost of money is an estimate of AA bond prices corresponding to the inflation rates. Stock dividend rates are those necessary for a small utility to obtain risk capital.

Results of Economic Analysis -- Several solar total energy systems employing north-south collectors were studied, using SOLSYS (Task 8.3). System costs were as presented in the Appendix. A single house was also analyzed, using the simplified economic analysis program described in the previous quarterly report. It was assumed that construction was complete at the time of analysis, at the costs stated.

Figure 6, shows the level annual revenue requirements per house as a function of the percent of fossil fuel conserved for a solar total energy system servicing 1000 detached homes. The corresponding revenue requirements for a single home consuming fossil fuel and electricity in the conventional, nontotal energy manner are also shown. Figure 7 also presents the costs of the various solar total energy system components.

The results are stated as level annual revenue requirements, and would appear to be unusually high unless this term is understood. The 1974 price for energy for the single house is $383.22 per year. The level annual revenue requirement for energy for this same house, assuming 3.5% inflation, a 6-% interest rate, and a 30-year interval, is $1424 per year. This is not the amount most householders would be willing to pay for their energy, as they do not customarily include energy costs in a bank financing plan.

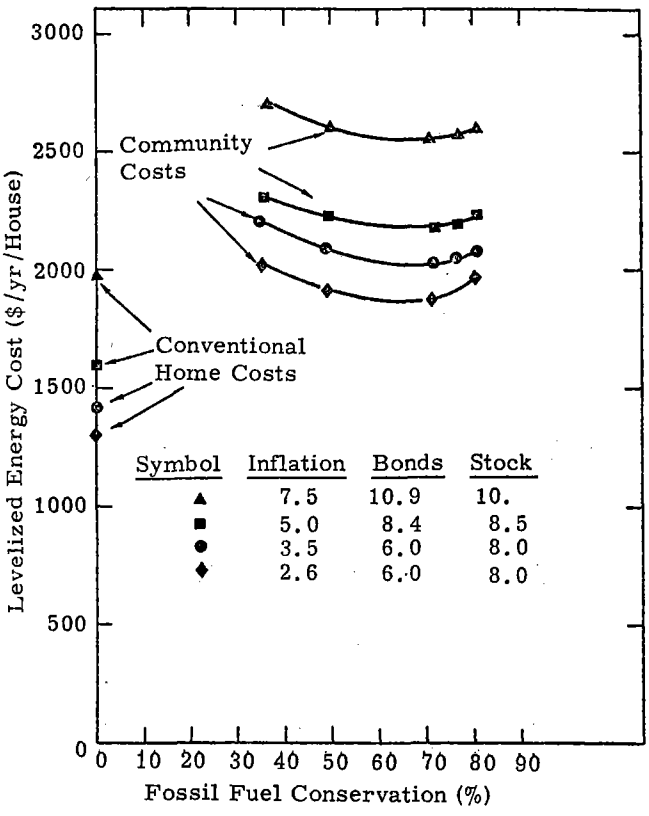

Figure 6. Comparison of Annual Levelized Costs for Conventional Homes vs Solar Total Energy Community, Albuquerque, NM (Assumes 30% conversion efficiency for electrical generation and 75% conversion efficiency for thermal requirements to compute fossil fuel needs of conventional system)

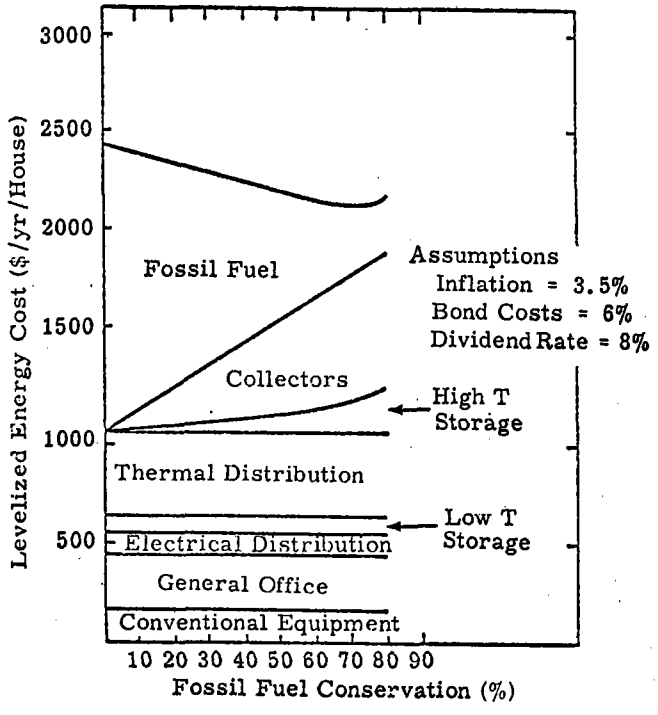

Figure 7. Cost Breakdown Solar Total Energy

The level annual revenue requirement is, however, appropriate in comparing dissimilar costs, as confirmed by several conferences with local utility people and other financial analysts. Although the values may appear high, in terms of current energy prices for a home the comparisons are valid, and reflect the relative financial advantages of the two systems being compared. Levelized analysis is the standard basis of comparison when costs occurring at widely different times are to be considered.

The cost comparisons shown above for Albuquerque, New Mexico, indicate that solar total energy systems constructed in 1974 would not be cost competitive. However, fast-changing fuel price structures will decrease this disadvantage. Albuquerque fuel prices are considerably lower than the national average, because of the availability of sufficient natural gas. Studies of other locations, with different system sizing for different loads, climates, and price structures, will show significant differences.

Task 3. Collector Field

3.1 Reflectors and Structure

The detailed design of the 200-m^2 field of east-west collectors has been completed and purchase orders for most of the parts have been placed. The collector field will consist of 20 of the 2.7 x 3.7 m (9 x 12 ft) units arrayed in four rows of five units each, with each row of five units forming a continuous 18.3-m (60-ft) trough assembly. Each pair of troughs will be aligned along an east-west axis with a 0.6-m (24-inch) gap between them for plumbing interconnections. North-south spacing between the two east-west rows will be 7.6 m (25 ft). The overall appearance of the collector field is shown in Figure 3.

Each 2.7 x 3.7 m unit consists of a thin shell structure 19 mm (0.75 inch thick) fabricated to the specified parabolic contour and mounted on a framework of five transverse ribs joined at their outer ends by longitudinal members (see Figure 8). The shell structure is produced in four shorter sections 0.9 m (36 in.) long, which are assembled and bonded to form the full-size shell. The shell is bonded to the rib framework which in turn is attached to a simple tubular steel frame with flat steel end plates. The end plates are bolted to flanges on the ends of the trunions on the pylons. Stress analyses of wind loads have verified design adequacy in both 13.4-m/s (30-mph) operational and 40.3-m/s (90-mph) survival situations.

Each trough assembly will be supported at the ends by a narrow pylon of welded steel sheet. The pylon height places the rotational axis of the assembly 1.5 m (5 ft) above the concrete bases on which the pylons are bolted. A prototype pylon has been fabricated and tested to significant overloads without damage. The concrete pedestals for the 200-m^2 field are presently under construction, along with other major portions of the system installation.

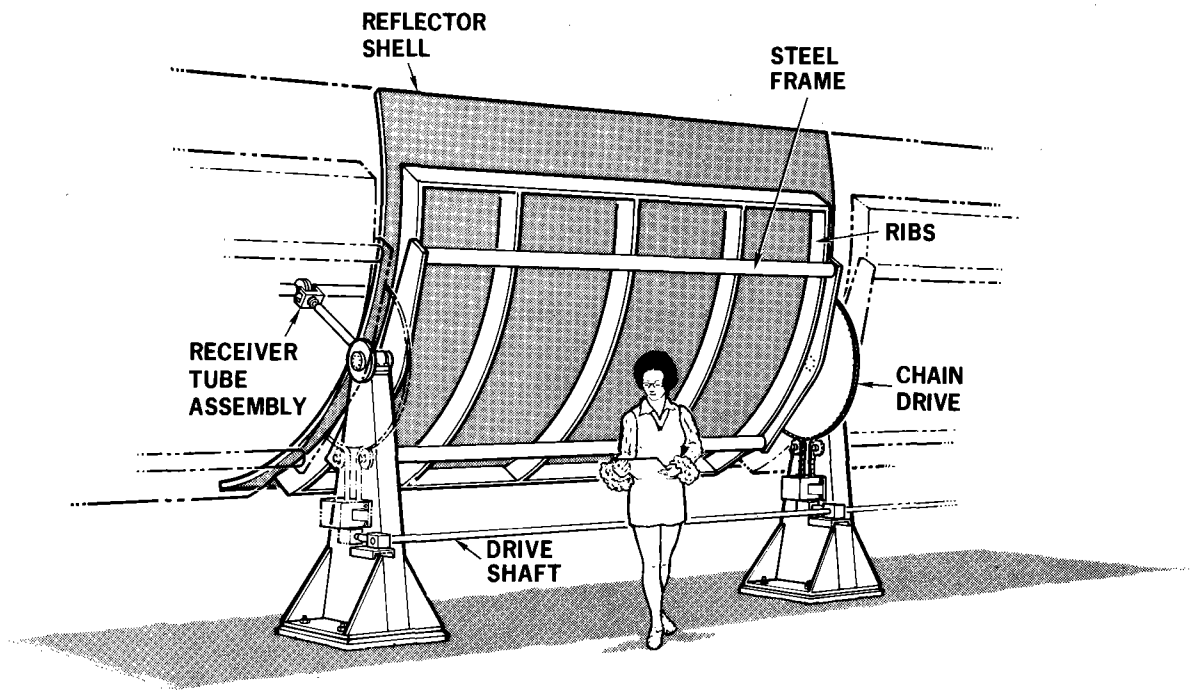

Figure 8. Reflector Trough Assembly

Though the overall design has been established, manufacturing details are still being worked out for the reflector shell structure. Twelve development models of the 0.9 x 2.7 m (3 x 9 ft) sections of the shell structure have been produced with slight variations in fabrication parameters These 12 sections are being evaluated to decide which version will be specified for the production units. Evaluation includes (a) the cutting of test specimens to determine mechanical properties, (b) painting with a water-repellant preservative and varnish finish as planned for production units, and (c) lining with reflector materials to determine the basic accuracy of the parts. Besides establishing fabrication parameters, these sections will be used to develop the techniques and facilities for trimming and assembling of the production units. (The decision on which manufacturing process to use for the 200-m^2 installation was made in late April.) Four of the 12 development models will be used to fabricate one prototype 2.7 x 3.7 m unit; this unit will be used to verify design definition and assembly techniques, then will be fitted with reflectors and mounted in a 45° tilt north-south frame for functional testing.

Drive System -- Although an entire 18.3-m (60-ft) trough tracks as a single structure, drive is provided by five separate sprocket and chain assemblies, two of which may be seen in Figure 8. The sprocket and chain assemblies are driven by a common drive shaft. Each unit of the trough is driven only at its west end, leaving the east end essentially free, but mechanical connections between adjacent units make the entire trough move as one.

The drive system for rotating each of the four 18.3-m (60-ft) troughs will consist of a single 1/6-hp, 50-V dc electric motor mounted on the pylon at the west end of the trough. A series of

line shafts and reduction gears provides the drive for each of the five sprocket-and-chain assemblies. The electric drive motor for each trough is rated at 1.13 N·m (10 in.-lbs) of torque at full load and full speed (1000 rpm). The gear reduction ratio of 50,000 to 1 between the motor output shaft and the trough provides a maximum tracking rate of 7.2°/minute. Torque is sufficient for operation in 13.4-m/s (30-mph) winds, with a safety factor of more than 3. The designs for the mounting and drive mechanisms consider the 3 mm (0.12-in.) change in length of each unit's steel framework over the expected outdoor temperature range, and the 10 mm (0.4-inch) maximum change in length of the reflector due to shell shrinkage and expansion caused by moisture.

Reflector Materials -- Development efforts aimed at incorporating the reflective material as an integral part of the trough shell structure have met with limited success. Fabrication techniques attempted thus far have resulted in acceptable and functional reflector surfaces but without the desired accuracy. The troughs with integrally molded reflectors produced to date are not of the required optical quality. Slope errors of up to 1.5° have occasionally occurred while errors of 0.5° are common. These errors are due to mold inaccuracy, uneven shrinkage of adhesives, impregnating resins or glues, warpage of the sheet material after fabrication, and combinations of these.

The degree of reflection inaccuracy can be illustrated by describing one inspection technique used with the two 2.7 x 3.7 m fiberglass-trough/Alzac-reflector assemblies. An asbestos-based sheet material was painted with a recurring series of stripes of temperature-sensitive prints centered on the focal line of the trough. When the board was placed in position in the focal plane and the tracker system activated, the reflected, concentrated solar energy illuminated the printed band and discolored the paints according to the temperature reached in a 30-minute exposure. Figure 9 illustrates the setup and the results. The primary reflected illumination fell within the diameter of the receiver tube, but some of the energy was obviously outside of the intended area. Photographs were taken but the high intensity of the illumination along the focal line made suitable film exposure virtually impossible.

Evaluation of integral reflectors on parabolic troughs indicated that a better means of applying reflector material was needed. On the basis of previous successful experiments with mechanical clamping of sheet reflector materials, it was determined that this approach would produce a more accurate, more acceptable reflector surface for the large troughs. The concept of mechanical clamping requires a separate thin sheet of material (such as a 0.64-mm (0.025-in.) aluminum sheet) which can be held or clamped so that it is forced to conform to the basic trough contour. The structural integrity of the sheet allows it to assume the basic trough contour smoothly as it is bent, thereby bridging the small irregularities of the trough surface. The primary method of clamping is to exert force on the edge of the sheet at the outer rims; the force direction is tangential to the parabolic slope at the rim. The separate reflector sheet must be slightly larger than the rim-to-rim arc length of the parabola; the extra length will be a function of the clamping device design.

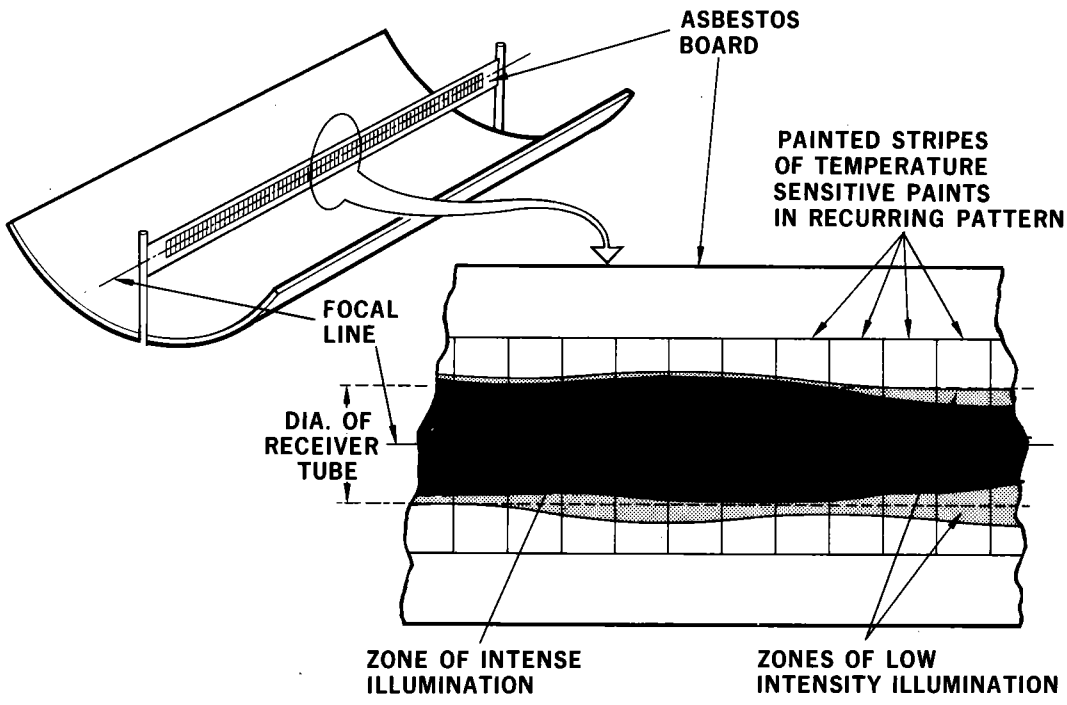

Figure 9. Determination of Reflector Accuracy

This approach of using a clamped structural sheet with a highly reflective material applied to it allows important versatility in the collector field design. Installation of the reflector material can be delayed until late in the assembly sequence, thereby eliminating the extra precautions which would otherwise be required to protect the reflector throughout fabrication and assembly. Replacement of a damaged or degraded reflector section of a trough can be easily effected with such a design. In a developmental solar collector field, this approach will permit easy substitution of new and better reflector materials as they become available.

The prototype shell/rib/frame trough structure being assembled will evaluate mechanical clamping of 0.64 mm (0.025 in.) Alzak reflector sheets. Provision has also been made to try 3.2 mm (0.125 in.) glass sheets which have been sagged to contour and silvered.

As a result of the work being done by the Sheldahl Company of Northfield, Minnesota, three promising film reflectors have been developed which can be applied (by adhesive) to a 0.64-mm (25-mil) aluminum sheet for mechanical clamping; they are:

Second-surface-aluminized FED Teflon

First-surface-aluminized Mylar with a protective polymer coating over the aluminum

First-surface-silvered Mylar with a protective polymer coating over the silver

All metallic reflector coatings are applied by metal evaporation in a vacuum chamber. These three reflector films have specular reflectance values of 0.80 to 0.89 as compared to Alzac's 0.70.

Present plans for the 200-m^2 collector field of Phase IV-A are to procure from Sheldahl sufficient quantities of reflector sheets (reflector film on the 0.64 mm aluminum sheet) to cover two of the four 18.3-m (60-ft) troughs with the second-surface-aluminized Teflon. The third trough will be covered with the first-surface-aluminized Mylar, while the fourth will use first-surface-silvered Mylar. Alcoa's Alzak reflector sheet will be a backup reflector material which could be mechanically clamped to the troughs if desired.

3.2 Receivers

The receiver tube design has been completed and is shown schematically in Figure 10. Fabrication of these units is in progress. Basically, the design consists of a selectively coated steel receiver tube with flanged ends. The receiver tube is enclosed in a glass envelope joined to the flanges, permitting evacuation of the annulus around the receiver tube. The metal bellows provided in the glass envelope compensates for thermal expansion and contraction. The entire receiver tube assembly is supported at the flanges by the two metal receiver tube support and expansion slides. The support holes in the flanges are slightly larger than the support slides to allow for movement of the assembly caused by thermal cycling. A hollow metal O-ring forms the seal between the flanges.

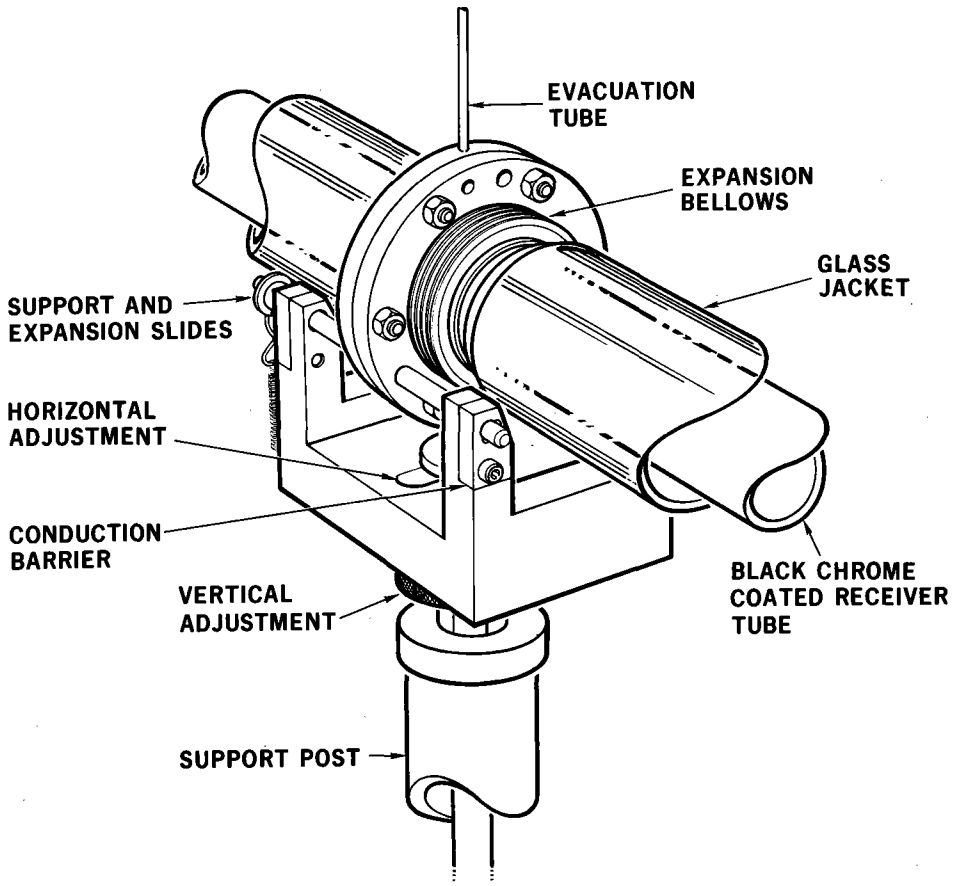

Figure 10. Receiver Tube and Support Assembly

Localized overheating of the fluid flowing within the receiver tube is prevented in two ways. First, the fluid is passed through no fewer than 10 collectors in series. This provides the high film coefficients accompanying the resultant high fluid flow rates; high film coefficients lower the probability of localized overheating. Second, a turbulence generator (i.e., an internal plug) within the receiver tube has also been used in the design. This provides high film coefficients and increased efficiencies at the low flow rates associated with low solar insolation. The limit of high flow rate has been chosen as that at which 1% of the collector field liquid energy gain is converted to the electrical energy necessary to pump fluid through the collectors.* Table III contrasts the relative merits of some design parameters.

TABLE III

Comparison of Design Features by Collector Efficiency
(all values in %)

	915 W/m^2 hr Normal Insulation (290 Btu/ft^2)		442 W/m^2 hr Normal Insulation (140 Btu/ft^2)	
	14.40 l/min Flow Rate (3.8 gpm)		4.80 l/mn Flow Rate (1.27 gpm)	
	No Plug	38 mm OD Plug (1.25 in.)	No Plug	38 mm OD Plug (1.25 in.)
No vacuum; insulation	53.14	55.30	40.73	43.66
Vacuum; insulation	58.08	59.85	49.82	53.15

2.7 x 3.7 m reflector, 90° rim angle, 41 mm OD receiver tube
(9 x 12 ft reflector, 90° rim angle; 1-5/8 in. OD receiver tube)

Absorptance = 0.95

Emittance at 500°F = 0.25
4.5 ms wind velocity (10 mph wind velocity)

Reflectance = 0.78
260°C T-66 temperature (500°C T-66 temperature)

Annulus Pressure 26.6 N·m^2 (0.2 mm Hg)

The annulus gap between the glass envelope and the receiver tube is nominally 9.5 mm (0.375 in.). Figure 11 presents the radiative, conductive, and convective heat losses from the receiver tube assembly as a function of annulus width. The trade-off that has been made in the selection of the 9.5 mm gap is as follows: as the gap decreases, radiation losses through the gap are only very slightly reduced (Curve B, Figure 11). However, if the vacuum in the annulus is lost and the gap fills with air, additional losses occur. Figure 11 indicates that the conduction and convection loss are at a minimum at about a 9.5-mm gap for temperatures from 200 to 315°C .

*The details of this approach are described in G. W. Treadwell, "Selection of Parabolic Solar Collector Field Arrays," SAND74-0375, Sandia Laboratories, May 1975.

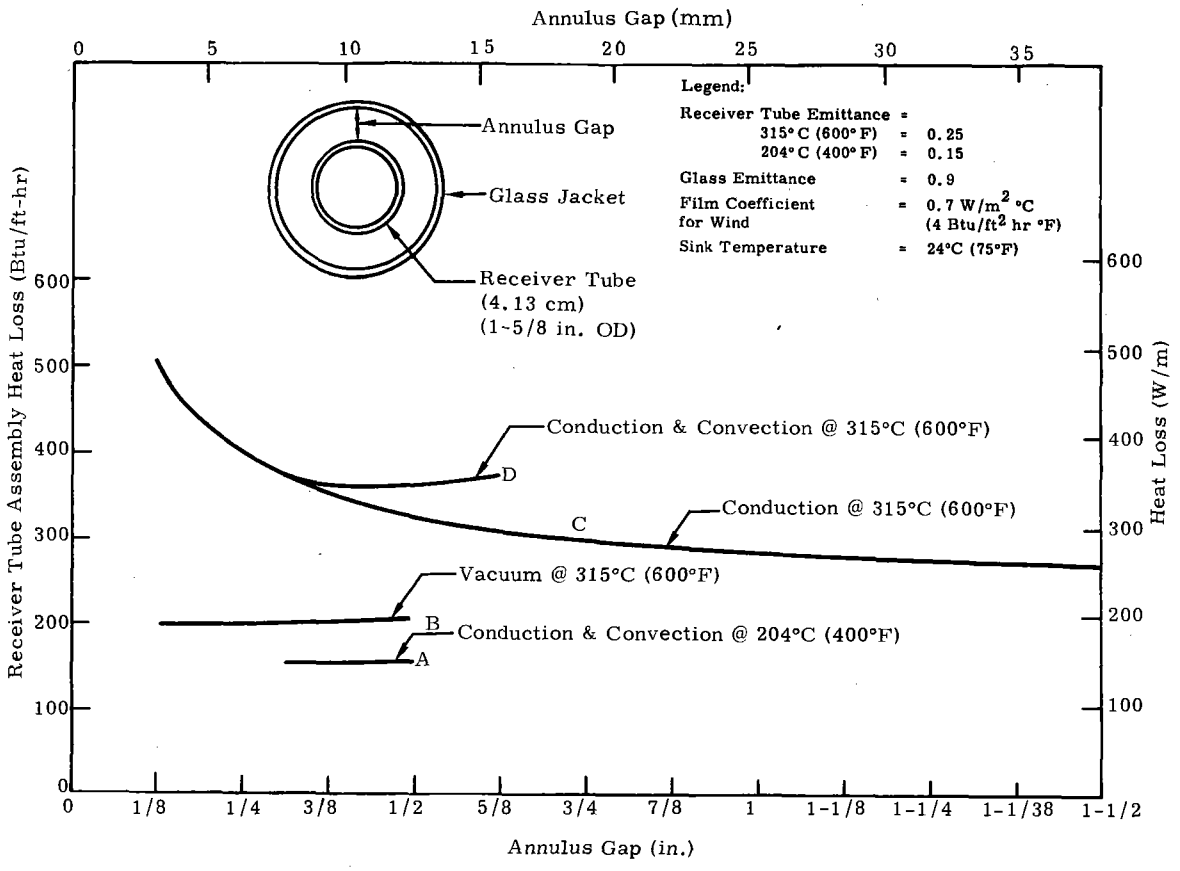

Figure 11. Optimization of Annulus Size

Therefore, the selection of this gap minimizes the consequences of a vacuum loss with only negligible sacrifice of performance when a vacuum is present.

3.3 Tracking and Control

The requirements for east-west and north-south tracking are very similar. Since the Solar Total Energy Test Facility will include collectors of both orientations, it was decided to design one tracking system for both. The requirements for the tracking system are as follows:

The tracking system should be flexible.

The system should have a tracking error of less than 0.1 degree.

The system should track both forward and backward.

The system acquisition angle should be 180 degrees.

The system should interface with computers.

The system should defocus automatically if power is lost.

The system should automatically shut down if sun is lost due to clouds.

System Evaluation and Development -- The tracking and drive system described in the last quarterly report was installed on two tilted north-south collectors at the collector test facility. Several months were spent in the evaluation of the tracking system resulting in the following modifications.

During the initial setup, difficulty was experienced in aligning the fine and coarse sensors; a smooth electrical transition could not be made from the coarse sensor to the fine. As a result, a single sensor is being developed. Adoption of the single sensor will allow simpler electronic design with reduction in cost of the total system.

The proportional control circuit was replaced with a switching-mode amplifier and current limiter because, during the initial evaluation, several motor drive transistors were destroyed. The switching-mode amplifier limits the starting current and operates the motor driver transistor in a safe current range.

Safety Features -- To insure that the receiver tube and the Therminol fluid do not overheat during a power failure, a power failure dropout relay will connect a battery to the collector drive motor. The collector will then be driven to the limit switch, out of any possible focus on the sun. Once the limit switch has been reached, the DC power circuit will be opened, stopping the motor until the limit switch and dropout relay have been manually reset.

To prevent receiver tube damage by overheating, thermocouples will be mounted on each string of tubes which will feed directly to the computer. Defocus will occur if the tubes get too hot.

System Operation -- The sun sensor output (Figure 12) is fed into the differential amplifier A1-U1. The balance control at the input of A1-U1 compensates for any current differences there might be in the two series photovoltaic cells used in the sun sensor as compared to the other two series photovoltaic cells. A1-U1 also has a variable gain control (fine gain) which can be varied 1 to 10. The output of A1-U1 is fed into an absolute value amplifier consisting of A1-U2 and A1-U3. The output of A1-U3 is always positive and represents a dc error signal which is proportional to any misalignment of the focused collector and the sun (see Figure 13). The error signal of A1-U3 is fed to A2-U4, a switching-mode amplifier, which in turn drives the motor drive transistor, Q11. A2-U4 acts as a current limiter with A2-U2. A2-U5 is a variable clock which can be varied from 1 to 60 seconds. The clock triggers A2-U6, which determines how long the motor is allowed to run during a clock interval. Q1 and Q2 are part of an inhibit circuit which applies a ground to the base of Q4 unless a positive pulse is at the output of A2-U6. A positive or negative dc signal is fed from the output of A1-U1 to A2-U1. If the input to A2-U1 is positive, A2-U7 will change states and cause Q8 to conduct, which causes the latching relay to change states. The output of the latching relay is 0 or 6 volts. If the output is 6 V, Q9 conducts, causing the reversing relay to change states and the motor will run in the reverse direction. A2-U3

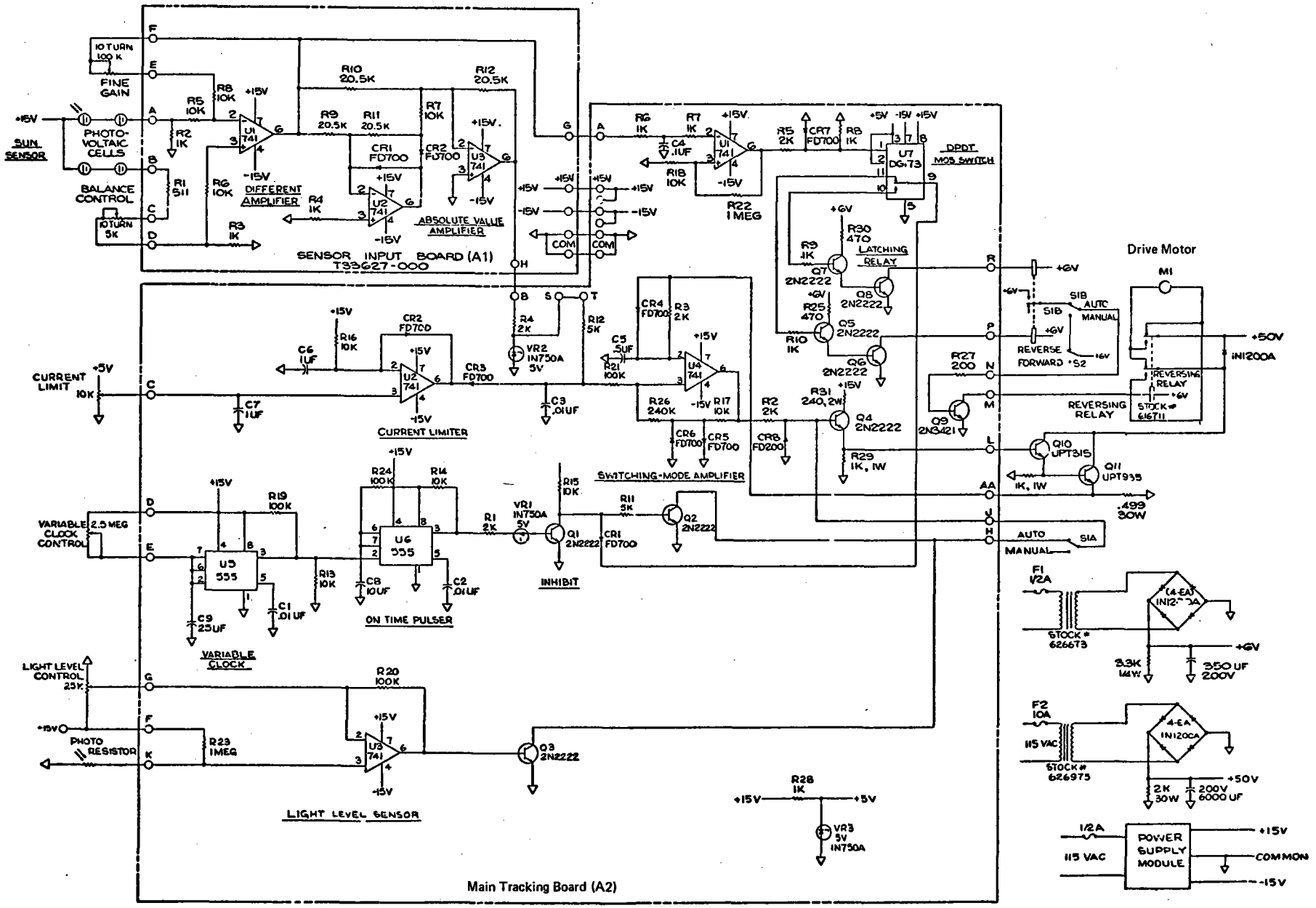

Figure 12. Collector Drive Motor Circuit

senses the sun's light level and applies a ground to the base of Q4 through Q3 when the light level decreases to a point where it would be inefficient to operate the solar system.

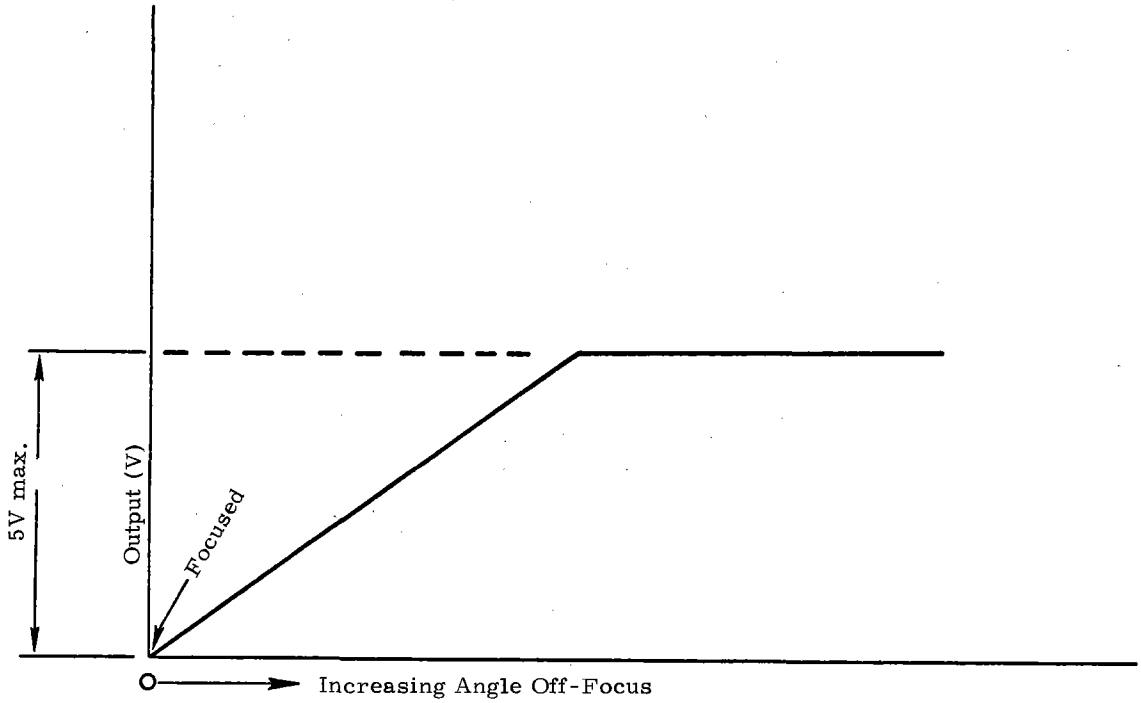

Figure 13. Error Signal Generated by Collector Misalignment

Future Development -- A temperature transducer sun sensor is being developed which operates on a principal of temperature difference rather than the light difference presently used. It is hoped that the temperature sensor will eliminate mistracking due to clouds and bright objects near the sensors. To make the temperature sun sensor operate properly, an automatic gain control (AGC) circuit will also have to be developed. The AGC circuit will enable the tracking system to operate with a slight haze or reduced sun intensity.

Collector Position Feedback and Digital Control -- To evaluate the performance of the analog solar sensors which provide input to the solar collector tracking servos, digital shaft encoders will be used to measure the angular position of the solar collectors. When fed to the minicomputer, these position data will enable the computer to monitor the functioning of the tracking servos and to alert the operator if a malfunction should occur. With digital shaft encoders the computer can, if necessary, generate the control outputs to command the drive motor circuits and steer the collectors independently of the analog solar sensors. Additional functions such as collector defocus, daily repositioning of the north-south collectors, and on-line monitoring of the collector drive system can be achieved expediently through computer software additions. The analog sensor approach is being evaluated and compared in cost, complexity, and performance to the digital shaft-encoder/computer method.

A block diagram of the digital approach to solar collector tracking is shown in Figure 14. In the present collector field layout, each encoder will be mounted directly on the axis of rotation of each set of five mechanically interconnected collectors. The selected encoder is a Baldwin 5V680BGL-1, 14 binary bit, single turn unit that provides a resolution of ±0.022 degree; this is within the pointing accuracy goal of ±0.1 degree. The internal construction of the encoder includes a Gray coded optical mask disk that carries the 14 concentric encoder segments. The Gray code is used because, between adjacent rotational segments, only one bit position changes so anomalous outputs that occur with natural binary segments are avoided. Internal circuitry standardizes the encoder's output to natural binary and to logic voltage and impedance levels that are compatible with the minicomputer interface. The encoder has a dust seal around its shaft and a rugged MS-type connector for environmental protection.

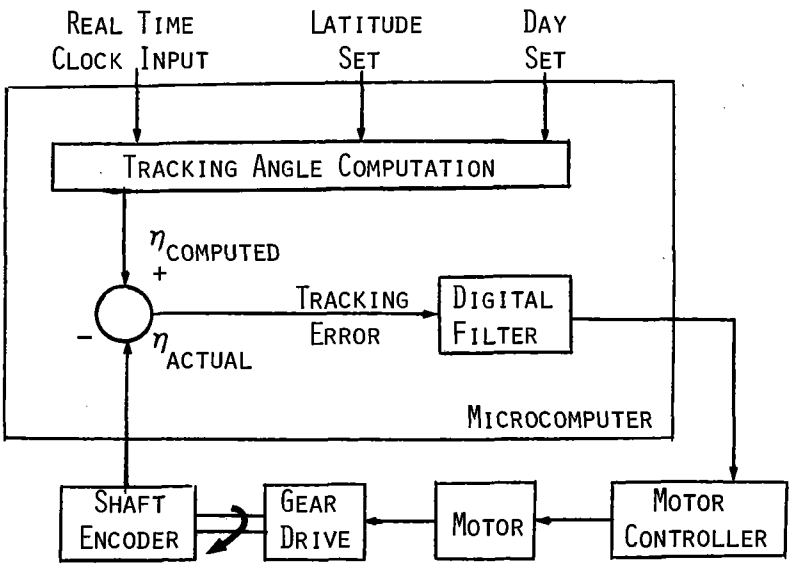

Figure 14. Computer Tracking Control

To reduce the amount of wiring from the minicomputer to the shaft encoders, the encoder-computer interface will include a multiplexer. This multiplexer is presently being designed and, when built, will be installed near the encoders.

3.4 Fluid Transfer System

The collector field primary requirements are as follows:

1. Allow evaluation of 2-trough collectors in series or 4-trough collectors in series to provide the required increase in fluid temperatures.
2. Control fluid flow rates using a variable speed pump instead of throttling flow with a valve; this minimizes pump energy.

3. So design system that fluid loop can be drained at night to minimize overnight heat loss. Present plans, however, are to not drain the system at night because of anticipated difficulties in removing nitrogen from pipe on a daily basis.

4. Provide a control buffer tank that can be used in either a mixing or blending mode.

5. Allow collectors to deliver heat to storage or to the cooler. Switching from one mode of operation to the other will be manual.

6. Provide for automatic cooling of storage, through system cooler, when storage is full. Collectors will not be turned off but will continue to supply storage at the rate storage is being cooled. Storage cooling rate must equal maximum solar collection rate.

7. Fully instrument system so that performance of all components can be monitored and evaluated.

To meet the requirements of the system, the collector field fluid transfer system is required to operate in the following five fluid flow modes:

1. All four trough collectors connected in series with the option of fluid flow direct to storage or to a cooler.

2. The collectors connected as two parallel strings of two troughs in a row with the option of fluid flow direct to storage or to a cooler.

3. The blending tank operating in the mixing mode.

4. The blending tank operating in the buffer mode.

5. The cooler operating to cool storage only.

The five modes are illustrated in Figure 15.

The field is designed to operate from commercial valve controllers under normal conditions. Initially, the computer will be used to help establish flow rate under complex conditions. It is anticipated that the controllers will be capable of performing the control functions of the computer and the goal is to arrive finally at a system that does not require computer control.

The problem of controlling fluid flow rate through the field is discussed in detail in Section 6. Control is accomplished using thermocouples at the input and output of each string of collectors. They provide information to the speed controller of the positive displacement pump so that a nominal collector field output temperature of 310°C (591°F) is maintained. Figure 16 is a control schematic of the collector field fluid transfer system. System control is provided by V7, a three-way control valve, which diverts the entire flow into the first collector when the four trough collectors are connected in series. When operating in the two-in-a-row mode, the valve splits the flow between the two parallel legs. The temperatures at points T1 and T2 are compared by a controller which drives the valve to keep the temperatures equal.

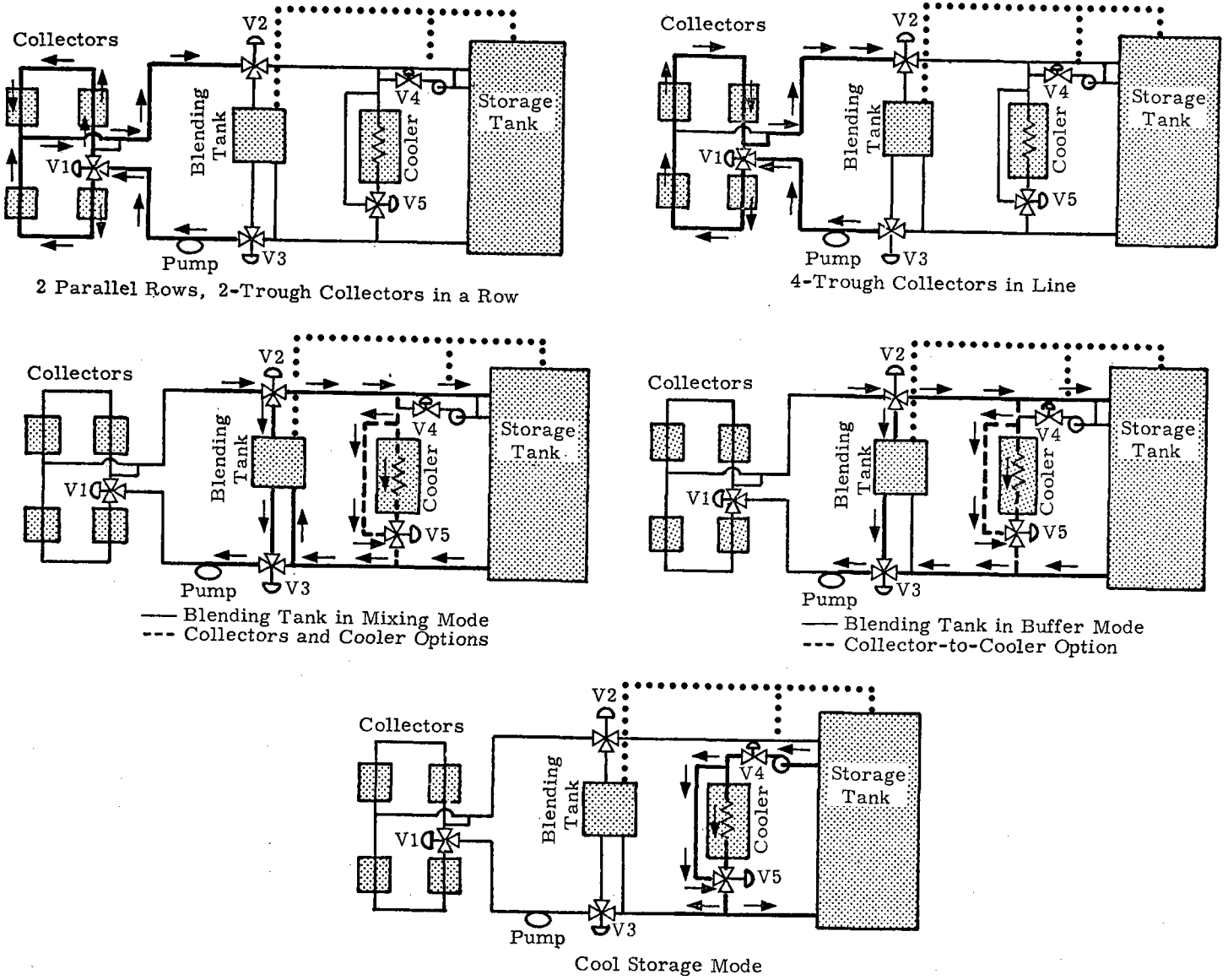

Figure 15. Collector Field Fluid Flow Modes

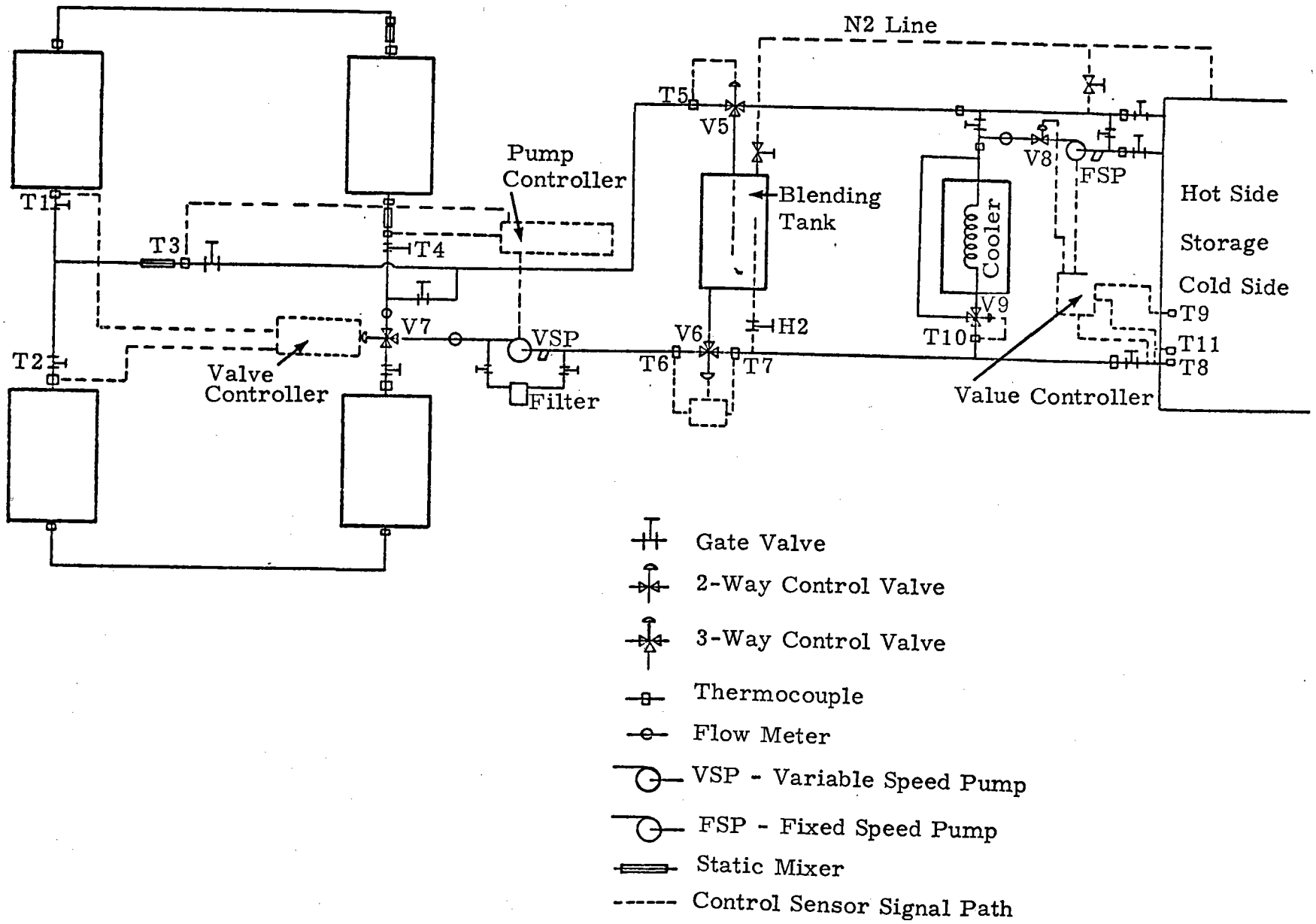

Figure 16. Collector Field and Storage Control

Thermocouples on the receiver tube outlets will sense the boundary layer film temperature of the heat transfer fluid. When the outlet thermocouples indicate the temperature is approaching the limit of 343°C (650°F), a safety sensor will defocus the collectors and accelerate the pump to provide maximum flow rate.

To enable the blending tank to operate in the mixing model, the three-way valve V6 opens fully from the blending tank and closes from the storage tank. It and valve H2 are in the open position.

When operating in the buffer mode, valve H2 is closed and valve V6 is used to modulate fluid from the blending tank so that it mixes with the fluid from the cold side of storage to the collector field.

The modulation of valve V6 is controlled by thermocouples before and after the valve and by sensing the liquid level in the tank. When the tank level is over the minimum allowable level, the control valve will open to keep the fluid to the pump 5.5°C (10°F) hotter or colder than the incoming fluid from storage. Fluid is diverted to the tank through valve V5 which switches all fluid not within temperature tolerances to the blending tank.

The pipeline size in the collector field has been increased from 1 inch to 1-1/4 inch nominal pipe. This was necessary because of the higher collector field flow rates required, since the ΔT of the fluid through the collector field has been lowered.

The valves, controllers, 1-1/4 inch carbon steel tubing, and insulation for the collector field have been ordered. Delivery is expected in June. The pump will be delivered at the end of July.

3.5 Cooler

The cooler shown in Figure 16 has a capacity of 1.055×10^6 kJ/hr (1×10^6 Btu/hr). Its purpose is to act as a thermal load on the system upon demand. The heated fluid returning from the collector field can be diverted to the cooler rather than to the storage tank; this allows the collector field to operate without affecting storage. When its pump and control valve V8 are activated, the cooler can cool the fluid in the upper portion of the storage tank and return it to the bottom.

If the storage tank should be completely filled with the heated fluid from the collector field, this fluid would be recirculated through the collector field. This would result in fluid overheating by the collectors, causing damage to both the collectors and the fluid. To prevent this, the cooler pump is activated and control value V8 is opened fully when the hot fluid reaches thermocouple T8 in the storage tank. The cooler will continue to operate in this manner until the level of the cooler fluid rises to thermocouple T9.

The temperature of the fluid leaving the cooler is regulated by the three-way control valve V9. The valve blends hot fluid from the bypass line into the fluid coming from the cooler to maintain the desired outlet temperature as sensed by thermocouple T10.

Before the cooler is started, the fluid in it and the bypass line are at ambient temperature. To prevent this mass of cold fluid from being introduced into the collector field abruptly when the cooler is started, a cooler preheat cycle has been added. As the level of the hot fluid moves lower in the storage tank and before it reaches thermocouple T8, thermocouple T11 activates the preheat cycle. This starts the cooler pump and sets the control valve V8 for a low flow rate through the bypass line. Control valve V9 will automatically block flow from the cooler until the fluid coming from the bypass line exceeds the set-point temperature of the valve. At this point, the bypass line is preheated and normal operation may begin.

The cooler will be a McQuay Company unit which has been ordered for delivery in August 1975. The pump will be a centrifugal type (Dean Brothers) with delivery expected in September.

Task 4. High-Temperature Storage

High-temperature storage for phase IV-A uses an insulated 2000-gallon tank which was originally designed as a storage test facility. Figure 17 shows the assembly, almost complete at the time of this writing. The unit is scheduled to be tested using both water (450° F) and Therminol 66 (600° F) as the storage fluid. This testing will be to determine thermocline stability, input/output fluid requirements, tank heat loss, fluid inlet diffuser design, fluid outlet vortex preventer design, and tank side wall conduction effects. Following completion of these tests, the tank will be installed at the test facility.

4.1 Storage Fluid Transfer System

Figure 18 is a basic schematic of the fluid loop. The system is designed to operated in three basic flow modes as shown in Figure 19. The basic requirements for the system are as follows:

1. Operate the boiler with the heat from storage.
2. Operate the boiler with the gas heater.
3. Switch automatically from 1 to 2 and vice versa, depending on condition of storage.
4. Add heat to storage with the gas heater starting with fluid at ambient or boiler-return temperatures (450+ °F).
5. Operate boiler and add heat to storage simultaneously with the gas heater when boiler is in partial load condition.
6. Allow full flow through the gas heater at all times to insure good heat transfer in the heater at all times.

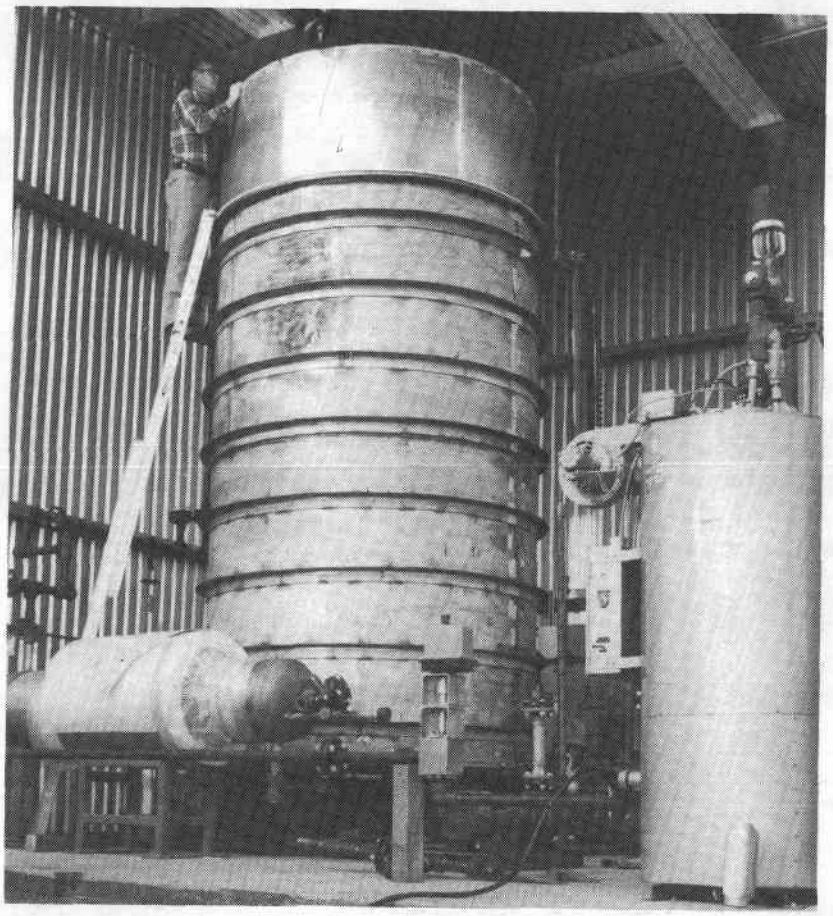

Figure 17. High Temperature Thermocline Storage Tank

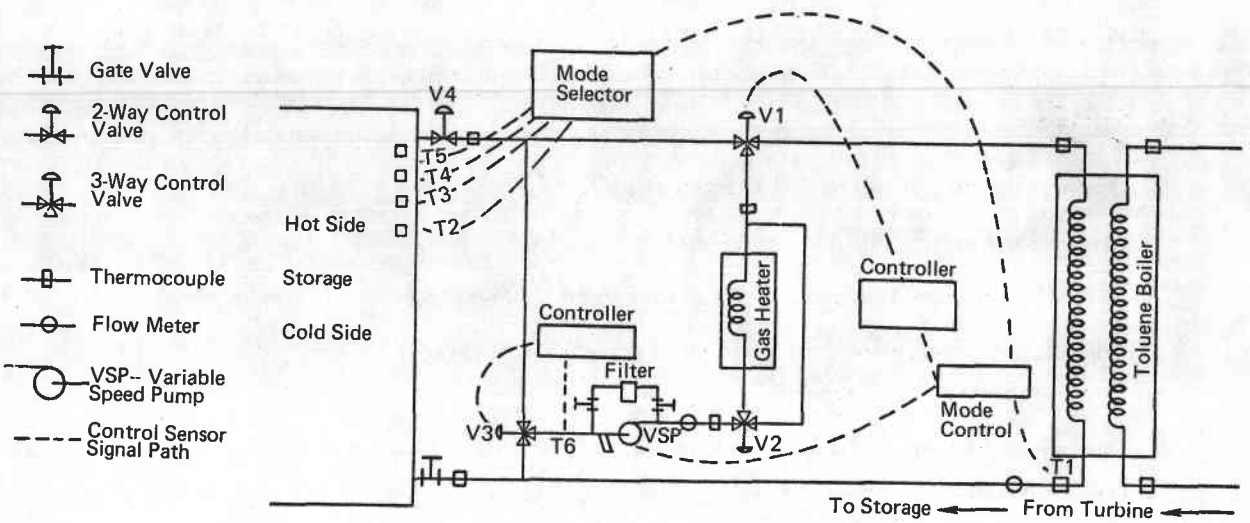

Figure 18. Storage Fluid Loop

In the storage-boiler mode, control is through thermocouple T1 (Figure 18) which controls the speed of the variable-speed pump (VSP). The fluid flow rate is adjusted to keep the temperature of return fluid out of the boiler constant so as not to disrupt the storage thermocline.

In the heater-boiler mode the VSP is operated at full flow and the boiler load is met by control of valve V1 by thermocouple T1; V1 diverts excess flow to storage or to a recirculation path through the heater, depending on the setting of valves V3 and V4.

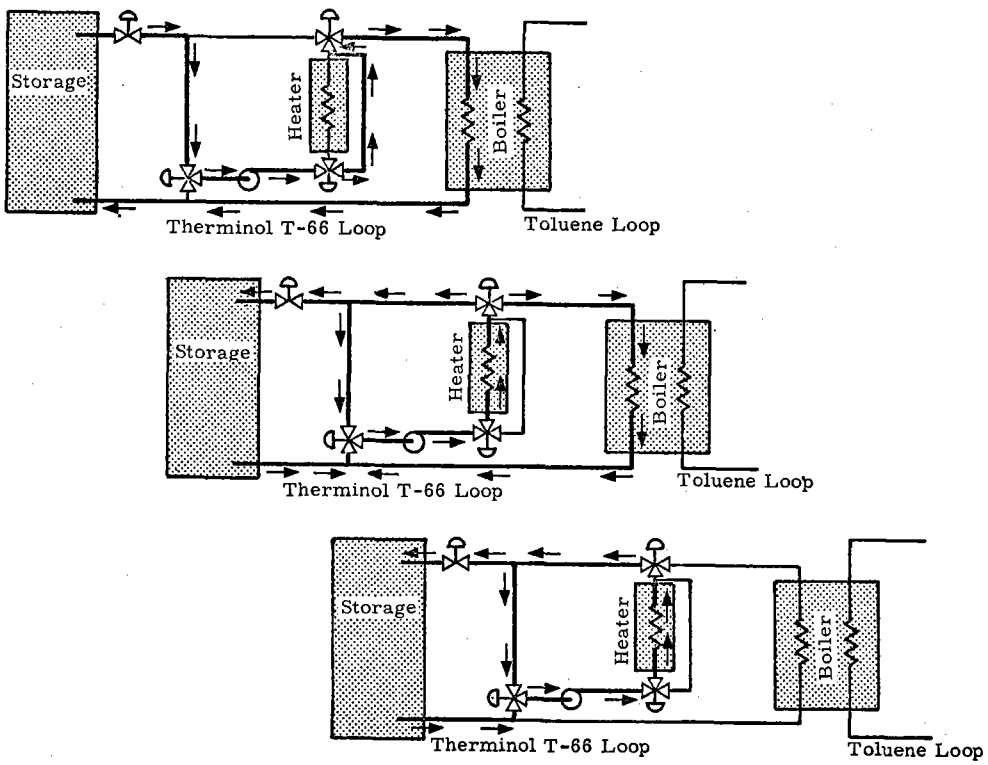

Figure 19. Storage Fluid Transfer System - Basic Flow Modes

Automatic switching from storage-boiler to heater-boiler mode and vice versa is through thermocouple sensors T2, T3, T4, and T5 in the storage tank. When operating as storage-boiler, the level of the thermocline moves higher in the storage tank. When it reaches thermocouple T4, (Figure 18) a gas-heater preheat begins. This consists of a low flame in the heater and valve V2 diverting a small amount of fluid through the heater. When the hot fluid level reaches thermocouple T5, the preheat cycle is complete and the system switches to the heater-boiler mode.

When operating in the second mode (center of Figure 19), the thermocline level moves lower in storage. As it passes thermocouple T3 (Figure 18) the heater bypass line begins its preheat cycle. This consists of valve V2 diverting a small amount of fluid through the bypass line. When the hot fluid level has dropped to thermocouple T2, the preheat cycle is completed and the system switches to storage-boiler mode.

For heat storage (bottom of Figure 19), full flow through the variable-speed pump is maintained and valve V3, controlled by thermocouple T6, is used to adjust flow going to storage. The variable-speed pump is not powerful enough to provide full flow through the heater with fluid at ambient temperature. The purpose of V3 and T6 is to blend hot fluid with ambient incoming fluid so its viscosity is low enough for the pump to maintain full flow to the heater.

Detailed design of the storage fluid transfer system is 50% complete and all long-lead-time items have been ordered, i.e., pumps, valves, valve controllers, flow meters, and instrumentation.

Task 5. Turbine/Generator System

5.1 Toluene Boiler

The heat exchanger to transfer the heat from the Therminol 66 (T-66) fluid to the turbine fluid is on order with delivery scheduled for June. The heat exchanger consists of four separate elements--one for preheating, two for boiling, and one for superheating. Each element is cylindrical and will be part of a continuous vertical stack when the exchanger is installed in the turbine room of the control building; mounting will be on four threaded rods attached to an overhead support. This arrangement was chosen to minimize conductive heat loss paths. With insulation by a 10.2-cm (4-in.) thick ceramic fiber blanket, heat loss from the exchanger will be less than 1/2% of the heat transferred.

5.2 Turbine

The order for the turbine/generator from Sundstrand Aviation is proceeding on schedule and delivery is expected in July. Performance predictions by Sundstrand indicate that cycle efficiencies will be somewhat lower than those in the initial system-sizing studies. In general, lower performance is a consequence of adapting an existing system to the solar total energy application. With the exception of the turbine wheel which was redesigned for application in the Solar Total Energy Test Facility, turbine system subcomponents such as pumps, condensers, and throttling valves will operate at flow rates and pressures different from those for which designed. A Rankine cycle system designed from the start for solar applications would not exhibit such lower performance. The changes in performance are as follows:

	Winter		Summer		Spring/Fall	
Condenser temperature (°C, °F)	73.9	165	93.3	200	48.9	120
	old	new	old	new	old	new
Cycle efficiency (%)	17.7	16.2	15.6	13.5	20.4	16.9
Storage ΔT(°F)	140	120	127	105	155	123

These changes in storage ΔT decrease the effectiveness of storage, increase the required T-66 pumping rate and work, and reduce collector performance.

During this reporting period provision was made to integrate the Sundstrand control system into the overall solar test facility control philosophy. The instrumentation for the turbine/generator and associated fluid piping loops has all been ordered. All of the deliveries have been promised before the end of June. The instrumentation categories involved are:

TEMPERATURES: turbine inlet, regenerator vapor inlet, condenser inlet, regenerator liquid inlet, condenser cooling water loop in, condenser cooling water loop out, toluene (CP-25) preheat input, CP-25 boiler input, CP-25 superheater input, CP-25 superheater output, Therminol input to CP-25 boiler and Therminol output from CP-25 boiler. FLOWS: regenerator liquid inlet, cooling water loop out, Therminol through heater and Therminol through boiler. PRESSURE: turbine inlet, regenerator vapor inlet, condenser inlet, regenerator liquid inlet, CP-25 preheat input, CP-25 boiler input, CP-25 superheater input, and CP-25 superheater output.

The instrumentation and control functions will be located in the control room to remove the operators from the noisy environment of the turbine/generator. Shielding conduit is being used for all of the instrumentation and control lines to the control room. Once these lines are in the control room, direct access will be available to the computer and other data processing equipment.

5.3 Rankine Loop Heater

The Rankine loop heater is used to heat the T-66 when sufficient thermal energy is neither being collected nor in storage. This is the natural-gas-fired heater used by Sundstrand to vaporize toluene in their total energy turbine package. The design application is for vaporizing toluene to the super-critical state at a rate from 317 to 3170 MJ/hr (300,000 to 3,000,000 Btu/hr). The current application is to heat Therminol at heat rates from 105 to 949 MJ/hr (100,000 to 900,000 Btu/hr). Consequently, careful attention is being given to the utilization and control of this heater because of the difference in applications. One particular aspect of concern is the avoidance of hot spots that could conceivably exceed the decomposition temperature of the T-66. During start-up, the maximum flow rate of T-66 is low and laminar flow will persist in the heater. Heat transfer during laminar flow is poor, potentially causing undesired hot spots. It is therefore necessary to provide recirculation to increase the temperature and Reynolds number enough to insure turbulent heat transfer.

Another item of concern is that the minimum flame setting of the heater is higher than the minimum desired in the solar application. None of these problems preclude the use of the heater but they do complicate the methods of use and control. A study contract has been placed with Sundstrand to determine heater performance under solar applications and to determine the feasibility and desirability of modifying the heater.

5.4 Turbine Heat Exchanger

The turbine load heat exchanger constitutes the interface between the condenser cooling loop and the cooling tower loop. This exchanger is to keep the cooling tower water, which becomes contaminated by the evaporation process, out of the condenser and low-temperature storage. A "Graham Heli-Flow" counterflow heat exchanger will be used. Capable of transferring 632,000 kJ/hr (600,000 Btu/hr), it is available for installation.

5.5 Cooling Tower

The air conditioner and turbine cooling tower, an induction-type cooler supplied by Baltimore Air Coil Inc., is capable of dissipating 2.1×10^6 kJ/hr (2×10^6 Btu/hr) with 36°C (96°F) ambient and 21°C (70°F) wet-bulb temperature. This tower utilizes the induction spray cooling concept and consequently does not require fans with their attendant noise. The basic cooling tower, cooling-tower pumps, and piping to run from the remote tower to the turbine building are presently available.

5.6 Load Bank

The load bank for the generator is a stepped resistor type with a capacity of 49 kW, 3-phase, balanced-load, 60-Hz, 480 volts with forced-air cooling. The steps are as follows:

Step Number	1	2	3	4	5	6	7	8	9	10	11
Capacity (kW)	10	10	5	5	5	5	5	1	1	1	1
Total (kW)	10	20	25	30	35	40	45	46	47	48	49

Any combination of these steps may be used. The load bank, which is currently available, has provisions for remote operation from the motor control center and a thermal cutoff in the event of overheating.

5.7 Condenser Fluid Transfer System

The condenser fluid loop is the fluid system that interconnects the turbine condenser, cooling tower water heat exchanger, and the low-temperature storage. The fluid used in this loop will be a 30% ethylene glycol/water solution. The requirements for the system have been established as follows:

1. Maintain constant cooling water output temperature from the organic Rankine cycle (ORC) system condenser regardless of system load. Have the capability of changing system control to maintain instead constant ORC fluid output temperature from condenser.

2. Use the cooling tower heat exchanger to cool storage, bypassing condenser when so doing.

3. Sense when storage is full and automatically divert flow to the cooling tower heat exchangers.

4. Have the capability of blending flow from cold side of low-temperature storage with flow direct from condenser to maintain any desired condenser supply temperature (needed when temperature of low-temperature storage is lower than desired condenser supply temperature).

This system has been included as part of the control building design and is presently under construction.

5.8 Cooling Tower Fluid Transfer System

This system is a conventional cooling tower water system and is presently being constructed as part of the control building. The system will be large enough to provide the cooling needs of the organic Rankine cycle system, and the absorption air conditioner simultaneously.

Task 6. Instrumentation and Control System

6.1 Control and Equipment Center

A 140-m^2 building is being constructed to house system components and control equipment. This building will house all major system equipment except the collector field, high- and low-temperature storage, and cooling tower. The building is presently under construction with completion scheduled for July.

6.2 Control and Instrumentation

System Control -- Overall control of the system is maintained by control of the fluid transfer systems. The fluid transfer systems will be controlled at three levels.

1. Commercial controllers represent the lowest level of control capability. Pump speed and flow control valve settings are varied by single-channel commercial or industrial controllers. These controllers vary the settings to achieve a constant temperature and most of them have proportional, integral (reset), and rate features.

2. Delta® Honeywell control-monitor equipment is the middle level of control. The Delta® system can be used to:

   a. change set points on the controllers,

   b. monitor process temperatures and flow rates,

   c. send alarms if any process variable is out of safe tolerance or a motor is not running, etc., and

   d. present slides of circuits which are in alarm mode.

3. The minicomputer, at the highest level of control, has the capability to change set points of the controllers through the Delta® system. The minicomputer can then control by algorithms. Thus, optimum control strategies or characteristics can be developed through minicomputer programs, eliminating the need for hardware modification or adjustment.

It will be the goal to control the system with the first two levels; the third level will be used for performance calculations Initially, however, some of the control for the collector field and thermocline storage will employ the minicomputer for ease in optimizing control stability and operating efficiency.

Turbine Controls -- The organic Rankine cycle (ORC) turbine being procured for the project is equipped with a control system that provides completely automatic operation of the ORC power-conversion system when toluene is used as the working fluid and when the natural gas-fired heater is the power source. A number of significant changes will be made to the turbine when the ORC system is incorporated into the solar total energy system, the most significant being the addition of the solar-heated Therminol 66 (T-66) loop. Other changes include use of the gas-fired heater for backup power as well as for preheating the sensible heat storage piping and T-66 during cold start-up. These changes, and the hardware necessary to implement them, significantly affect the control of the ORC system.

Where necessary, the controls of the ORC system will be modified to accommodate operation with the solar heated T-66. To assure stable, efficient operation of the solar-powered ORC system, a computer model is being developed which will simulate the transient and steady-state response of the system in its various modes of operation. Presently, the ORC components such as the turbine band valve, turbine, regenerator, condenser, feed pump, and flow control valve can only be effectively modeled as empirical transfer functions. A contract to derive these models has been placed with Sundstrand since they have the necessary test experience and facilities to generate the required data.

Models of the Sundstrand heater and the T-66 to toluene boiler will also be developed by Sundstrand. These models are presently needed to address the initial design and control strategies

for the various modes of operation of the storage fluid transfer system. The Sundstrand model data will also be integrated into an overall system simulation that starts with the sensible heat storage tank and ends with the electrical and thermal output loads of the ORC.

When system testing is underway, comparisons will be made between the performance of the hardware and the simulation model. Refinement of the model will then permit further analysis and simulation for the purpose of optimizing the performance of the total system.

Collector Field Control -- Several new control strategies for the collector field start-up have been examined using the analytical model contained in the computer program CONTRL. The basic philosophy of the control strategies is best described by Figure 20. The control input to the field is the flow rate, that is, the output temperature of the field is controlled by adjusting the flow rate. The controller examines parameters in the field (such as field output temperature, solar insolation, or midfield temperature) and uses these parameters in conjunction with the output temperature set point to determine proper flow adjustments.

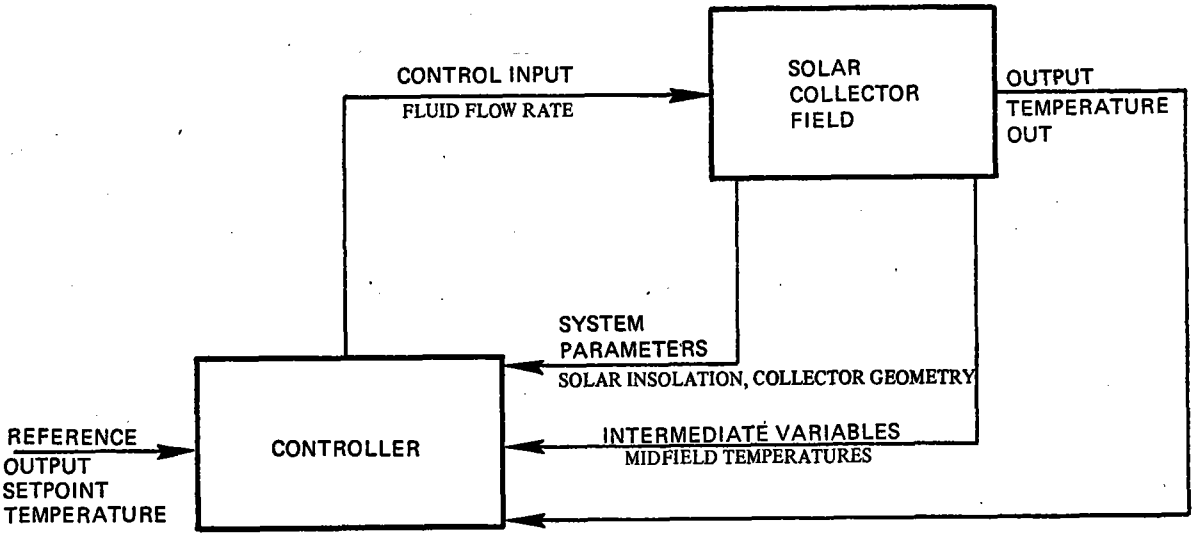

Figure 20. Basic Closed Loop Solar Control System

The first control strategy tried was discussed in the previous progress report and used proportional control based on output field temperature only. This strategy was extended during this reporting period to include information from the sun, that is, both the output temperature and the

solar insolation were used in the control algorithms. Improved stability during start-up resulted from this additional control information, but the results did not appear optimum.

This strategy was further expanded to include a feed-forward temperature from the middle of the collector field. Increased anticipation was the primary reason for using a midfield temperature. For systems which have long transport delays (such as the solar collector field), increased anticipation usually increases controllability. The control strategy was then applied to the flow arrangement in which recirculated collector field fluid is mixed continuously into the main line with lower temperature storage fluid during start-up, using a small mixing tank in series with the main fluid input line. The result was a transient response of the output fluid of 1 to 2% overshoot with a delay time of about 8 minutes (see Figure 21). Compared to the results of the previous report, the feed-forward/feedback control strategy considerably increases controllability. The control system was then programmed to determine the ability of this strategy to handle an abrupt change in solar insolation. As can be seen from Figure 22, the abrupt change in insolation did not cause an instability in control and the strategy responded satisfactorily.

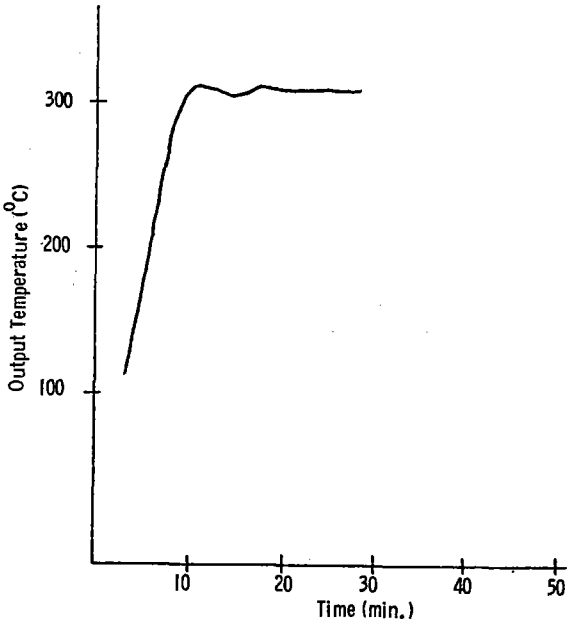

Figure 21. Transient Response of Fluid Temperature at Last Collector for 8:00 A.M. Start-Up in June

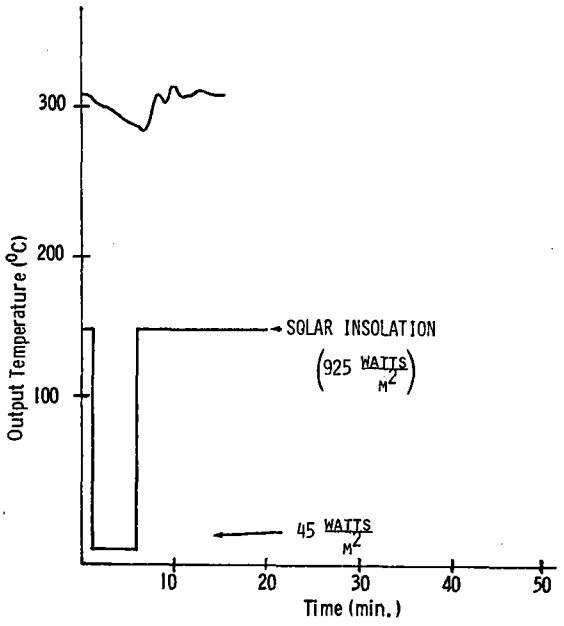

Figure 22. Transient Response of Output Fluid Temperature for Noon Solar Interruption in June

Instrumentation -- All of the instrumentation points in the system have been identified and instruments ordered. All of the minicomputer and Delta® control-monitor equipment has been ordered or received.

Delta presentation from all instruments will be as follows:

1. All instrument outputs will be recorded on computer-compatible magnetic tape.
2. Instrument outputs required for operation will be presented on digital meters.
3. Instrument outputs required for analysis of rapidly changing transient conditions will be presented on continuous chart recordings.
4. Any outputs desired may be printed out on the minicomputer control terminal.
5. Any plots desired may be made on the minicomputer control terminal.
6. Further analysis may be made at a later time by playing back the magnetic tape to either this system or the larger scientific computers.

Task 7. Collector Test Facility

The evaluation of receiver tube design characteristics in the test facility using a 1.2 x 1.8 m (4 x 6 ft) collector is more than 50% complete. The testing reveals that significant improvement in efficiency can be achieved with selective coatings. One selective coating remains for evaluation: black chrome over dull nickel with a reported $\alpha = 0.97$ and $\epsilon_{315°C} = 0.28$. It is expected that this black chrome will be equal to or better than the aluminum-molybedenum oxide-aluminum (AMA) coating on bright nickel.

Improvements have also been achieved through evacuation of the glass tube-receiver tube annulus. In addition, an insulating strip on the glass surface away from the reflector results in a significant efficiency improvement for the high-emittance coating. Computer codes have been developed which accurately predict these improvements. Some of the test results are shown in Table IV.

Same-day comparisons were typically conducted as consecutive data points to minimize the influence of the external environments. One comparison, the effect of internal receiver tube turbulence generators (plugs) cannot be conducted on the same day because of the time required to emplace and remove them. Differences from consecutive-day testing may be masked by changes in the weather. The computer models predict a 4.7% collector efficiency improvement through the use of plugs, but many days of testing may be required to verify the improvement.

TABLE IV

Average Collector Efficiency Percentage at 316°C (600°F)

Receiver Tube Coating	Design Feature: No Vacuum	Vacuum	Vacuum with Insulator	Vacuum with Plug	No Vacuum w/Plug	Remarks
Pyromark (Tempil) (α = 0.98, ϵ = 1.0)	16.2	18.3	23.9	x	x	Average of 5 days data for vacuum/no vacuum. Average of 4 days data for vacuum w/insulator.
Intermediate Black Chrome on Bright Nickel (α = 0.88, ϵ = 0.24)	32.1	34.6				Average of 8 days data.
AMA (Honeywell) (α = 0.97, ϵ = 0.38)	39.0	43.1	42.2			Average of 5 days data. Vacuum w/insulator 1 day average
Black Chrome on Sulfamate Nickel (α = 0.97, ϵ = 0.28)	x	x				

NOTES:
1. Volume flow rate approximately 5.7 l/min (1.5 gpm), Re > 12,000.
2. Test temperature varied between 302 and 311 °C (575 and 591 °F).
3. Collector efficiency percentage $= \dfrac{\dot{m}\ C_p(T_{out} - T_{in})}{(\text{aperture area})(\text{direct insolation})}$.
4. Direct insolation range 874 to 990 W/m^2.
5. Wind velocity range 0.24 to 1.7 m/s (0.78 to 5.57 ft/s).
6. Internal cylindrical plug of 16 mm (5/8-in.) diameter.
7. x = to be tested.

Task 8. Improved Data Base Compilation

8.1 System Load Profiles

The composition of a representative 2000 dwelling unit community has been defined. In addition, the electric load data for typical building types found in a community has been improved. HLOAD* is being used to compute the loads of the community.

Computer Load Programs -- An error in the Sandia CDC 6600 computer system routines has prevented the use of BLDGN* for the computation of thermal loads for the multizoned buildings found in the mixed-load community. The error, causing erroneous load computation, has been

*J. A. Leonard and S. Thunborg, "Solar Total Energy Program Quarterly Report, July-September 1974," Sandia Laboratories, SAND74-0391, December 1974.

isolated and corrected. Verification of the loads computed by BLDGN is underway. To allow the continuation of analysis, HLOAD has been modified to include loads due to occupancy and appliances. All buildings are thus assumed to consist of a single thermal zone. This assumption will be tested when verification of BLDGN is complete.

Mixed-Load Community Definition -- A flexible community description, incorporating statistical architectural data, has been prepared with the aid of the Architectural Department of the University of New Mexico. The data was compiled by Mr. Floyd Strub as part of a Master's Thesis published in May 1975. The community contains a total of 2000 dwelling units and is subdivided by building type as shown in Table V. Each subdivision is considered an independent subset of the community (e.g., low-rise apartments) complete with its own thermal energy distribution system. All subdivisions are connected to the central solar power facility by a single common thermal distribution pipe.

TABLE V

Definition of 2000-Dwelling Unit Community

	Structures	DU per Structure	DU per Acre	Floor Area per DU	Percent of Community
I. Residential					
Single Family Detached	504	1	6	139 m^2 (1500 ft^2)	25
Single Family Attached*	160	5	10	116 m^2 (1250 ft^2)	40
Low-Rise Apartment*	48	10	20	103 m^2 (1104 ft^2)	24
High-Rise Apartment†	4	54	54	114 m^2 (1225 ft^2)	11
II. Schools					
Elemetary	2	-	-	2529 m^2 (27225 ft^2)	
Junior High	1	-	-	2453 m^2 (26406 ft^2)	
High School	0	-	-	-	
III. Commercial	1	-	-	14864 m^2 (160000 ft^2)	
IV. Total Community Floor Space				259295 m^2 (2.79 x 10^6 ft^2)	

*Two stories
†Thirteen stories

Employment of a subdivision concept is important in that it provides facility for analysis:

- Isolated parts of the community such as high-density residential areas may be independently analyzed.
- Community design may be easily modified by changing the relative location and size of various subdivisions.

- Change in subdivision size is readily handled since each subdivision is complete and independent.

The total thermal energy requirements, for example, of a subdivision containing 72 low-rise apartment structures would equal 1.5 times that of the base subdivision containing 48 structures (see Table V). It would not be necessary to redefine the physical properties of the structures nor the thermal distribution system. Once the thermal requirements of the base subdivisions listed in Table V are known, any different size subdivision is defined through multiplicative operations. New communities may then be constructed by summing the thermal energy requirements of the newly sized subdivisions.

The UNM Architecture Department is currently preparing renderings of this community concept with particular emphasis on architectural integration of collectors and building design. A preliminary sketch of a multiuse shopping/residential complex supporting both east-west and north-south collectors is shown in Figure 23.

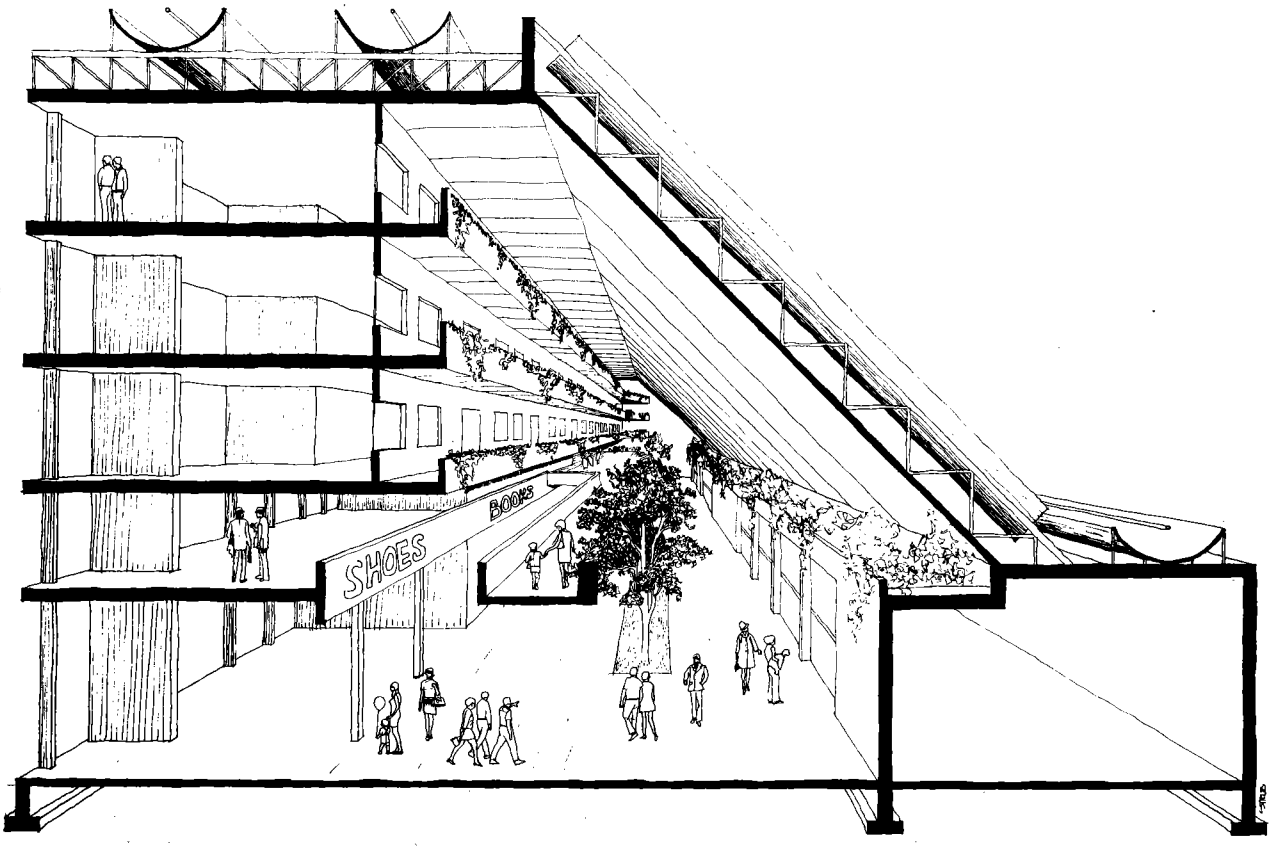

Figure 23. Solar Powered Commercial/Apartment Complex

Electric Load Data -- Following initial reduction of the 474-home residential subdivision electric load data provided by the Public Service Company of New Mexico, it was learned that a well and booster station of the city water system were being serviced through the same feeder line serving the residential subdivision. Six electric-driven water pumps are located at this station and they consist of the following: two 200-horsepower (149.2-kW) pumps, one 250-horsepower (186.5-kW) pump, and three 350-horsepower (261.1-kW) pumps.

A mathematical filtering technique was developed which sets out each step change exceeding 112 kW in power consumption between adjacent 15-minute segments. These step changes were arbitrarily assumed to represent a pump or pumps being switched on or off. This information was then transformed into a running schedule of the six pumps. This running schedule was used to extract from the original power consumption a power level equivalent to the pumps in operation during each time interval. This procedure has been carried out on four 1-month periods to define net residential electric power histories for the four seasons. The extracted pump power consumption and schedule were compared to monthly Public Service Company billing records and run-time logs at the pump station. This confirmed that the filtering technique provided electric load data representative of actual residential use.

Loads from three facilities in the commercial category have been combined with this single family residential load to represent the mixed load for the 2000-dwelling community discussed above. The three commercial facilities represented in the mixed load include high-density apartment housing, public schools, and a retail sales facility.

Where load demands of individual commercial and industrial customers exceed a given consumption level, the Public Service Company of New Mexico customarily provides a continuous recording of the electric power consumption. Records of this type for a 292-unit apartment complex, a 3100-student high school, and a 11,150-m^2 (120,000 ft^2) combination grocery/general-merchandise retail sales facility were provided by the Public Service Company of New Mexico. All three of these facilities are of recent construction. The data generally spans the 1973 calendar year. The data for each facility were reduced to provide an average diurnal load cycle on a unit area basis. This data is input to the SOLSYS computer program as part of a catalog of electric load data on various community facilities.

8.2 Solar and Weather Data

Focusing solar collectors use direct beam radiation. Unfortunately, measurements of direct insolation have only been made at a few U.S. locations, and even these data are intermittent and of questionable quality.

Since measurements of total (direct plus diffuse) insolation on a horizontal surface have been recorded regularly at about 75 stations, a formula which expresses direct normal radiation in terms of total radiation and/or other parameters would be very useful. Quite a few formulas for direct insolation exist. However, most are for clear sky conditions only, and some use independent variables which are not readily available, such as atmospheric turbidity.

One type of formula in particular is worth noting. This is the formula presented by Jordan and Liu* and Aerospace Corporation.† The formula is based upon the fact that the relationship between direct normal insolation and percent of possible insolation is somewhat linear. The Aerospace formulation is

$$I_{DN} = \begin{cases} A \cdot PP + B, & \text{if } PP \geq 25\% \\ \text{Zero}, & \text{if } PP < 25\% \end{cases}$$

where

I_{DN} = intensity of direct radiation on a normal surface,

PP = $I_{TH}/I_{EXT,H}$ is percent of possible,

I_{TH} = intensity of total radiation on a horizontal surface,

$I_{EXT,H}$ = intensity of extraterrestial radiation on a horizontal surface,

and A and B are the simple linear regression coefficients.

This formula, while easy to use, has several drawbacks. The linear regression equation seems to vary with time of day and with season. Furthermore, under partly cloudy conditions, there is no simple relationship between I_{DN} and PP.

Thus, it was decided that a formula should be developed which takes into account (1) seasonal variation, (2) diurnal variations, and (3) the scatter in I_{DN} values under partly cloudy conditions.

The first step was the selection of four 1-week samples of solar insolation data representative of the four seasons in Albuquerque. The samples were selected from March, June, September, and December 1962. The total radiation in each sample week equals the long-term weekly average of total radiation for that season. Both the direct- and total-insolation charts for these weeks were carefully digitized at 10-minute intervals.

These data were used to develop an estimation technique. Each week was divided into four time periods: early a.m., late a.m., early p.m., and late p.m. In each period the frequency distribution of I_{DN} as a function of PP was tabulated. Also, for each week those data points (PP, I_{DN}) which seemed to lie on a line were used to compute a linear regression equation.

---

*R. C. Jordan, and B. Y. H. Liu, "The Interrelationship and Characteristics Distribution of Direct, Diffuse and Total Solar Radiation," Solar Energy IV (3), July 1960, 11. 1-19.

†Aerospace Corporation, "Solar Thermal Conversion Mission Analysis; Vol. III, Southwestern United States Insolation Climatology," Report No. ATR-74(7417-16)-2, Vol. III, Prepared for NSF/RANN, November 1974.

This information was used to construct four seasonal formulas which use time and PP to estimate I_{DN}. One such formula is described in Figure 24 and illustrated in Figure 25. Note that several decisions are involved in each estimate. Variation in PP values is used to determine cloud conditions.

In order to estimate I_{DN} values for a date between seasons the two adjacent seasonal formulas and linear interpolations are used.

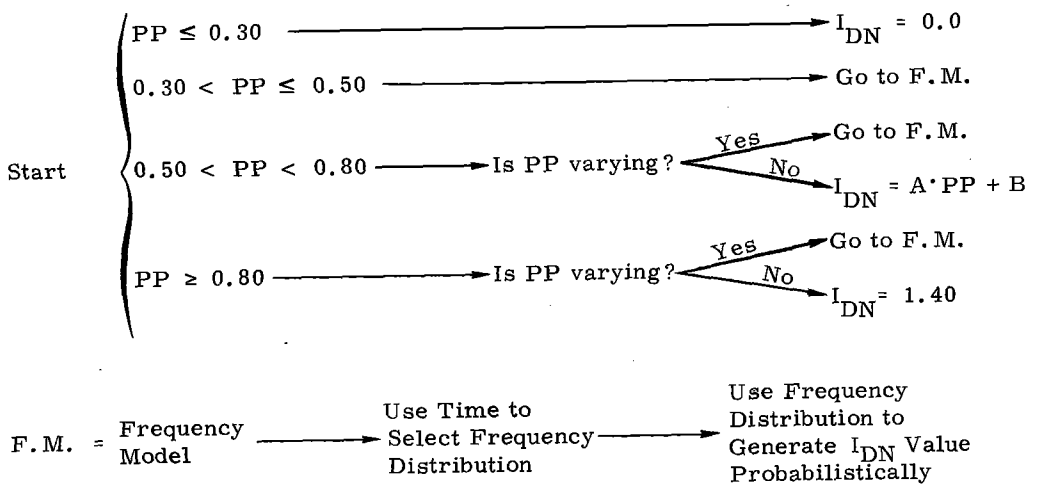

Figure 24. Solar Intensity Estimation Formula for June, Albuquerque

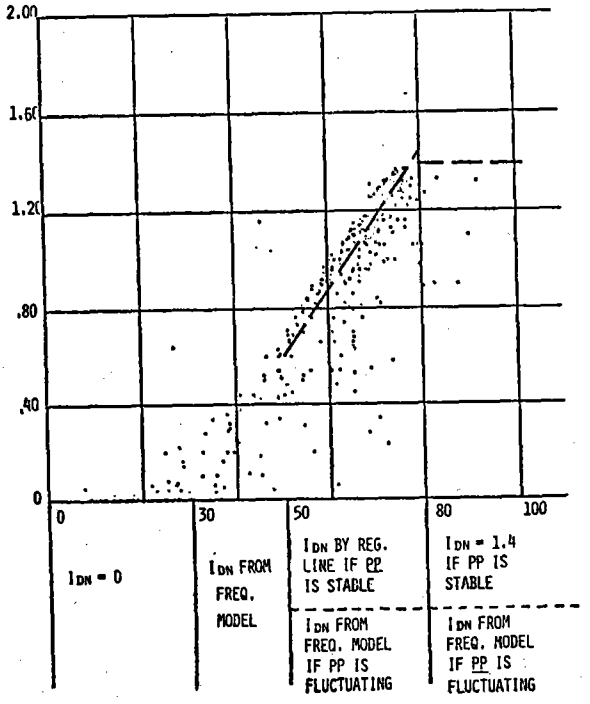

Figure 25. Illustration of Solar Estimation Formula for June, Albuquerque

Comparisons of these estimated values with actual data have been made. Figure 26 gives illustrations for both partly cloudy and clear days. During 11 days in May 1962, the integral of the estimated I_{DN} values was 4% above the integral of the actual I_{DN} values, while for 17 days in July the difference was 0.5%.

Plans for future work include further comparison and refinement as well as testing and modifying the technique for other locations.

These techniques will be used to estimate the necessary direct insolation data for seven of the eight cities chosen for analysis: Boston, Fort Worth, Los Angeles, Miami, Nashville, Omaha, and Seattle. Some of these cities, such as Omaha, Nebraska, have recorded insolation data which will provide verification of the technique.

Since Albuquerque (the eighth city being studied) has recorded direct and total isolation data available for 1962, these data, digitized at 10-minute intervals, will be used directly. Eleven months of recorded data has been digitized and is being adjusted for calibration errors. In addition, gaps in the data record will be filled and these along with questionable data will be flagged.

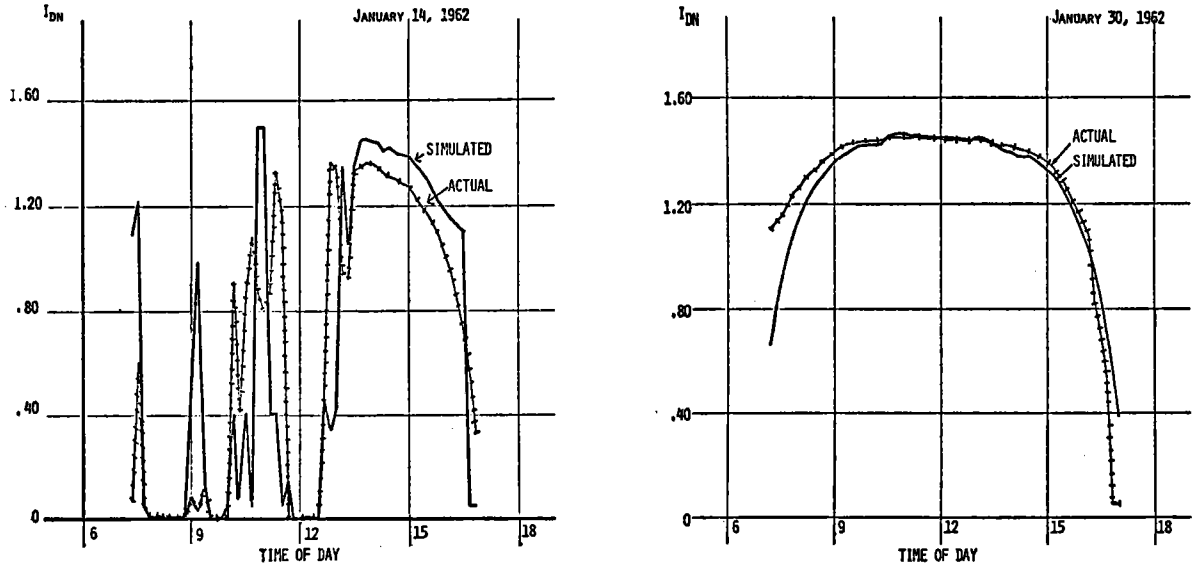

Figure 26. One-Day Comparison of Actual and Simulated Values of I_{DN}

Weather data for each of the eight cities have also been obtained and been converted to SI units, and are available on magnetic tape (see Task 2.2). These data together with the above four sample weeks of insolation data are being used in the systems analysis efforts.

8.3 Alternative Total Energy Systems

The program SOLSYS has been used to analyze the application of the solar total energy concept to a 1000-home community. This analysis effort is being expanded to mixed-load communities such as that described in Task 8.1.

1000-Home Solar Total Energy Community -- The analysis of the application of the solar total energy concept to a community comprised of 1000 separated single-family houses has been completed. This analysis was begun during the last reporting period and the guidelines are described in detail in the July-September 1974 Quarterly Report. Specific areas of analysis completed during this reporting period are:

- Inclusion of east-west horizontal cylindrical parabolic collectors.
- Parametric studies on the effect of changing collector area.
- Inclusion of actual recorded direct-beam and total insolation data for Albuquerque for 1962.
- Economic analyses of the solar total energy concept.

A comprehensive report* of this system analysis is being prepared for publication during the upcoming reporting period.

Table VI presents a summary of the performance of the primary components for each of the collector areas for the north-south 35° collectors as well as the east-west collectors. Furnace 1 represents, on the average, the amount of auxiliary fossil fuel required per day to provide the high-temperature fluid needed to generate electricity. Thus, increased collector area results in increased fuel conservation. The energy dissipated in tower 1 reflects the amount of excess high-temperature fluid energy (that required for electrical generation) dissipated in the cooling tower because the capacity of the high-temperature storage tank (storage 1) is exceeded. Similarly, furnace 2 and tower 2 represent the corresponding systems components for the low-temperature loop providing thermal energy to the thermal distribution system. Note that these latter two components respond independent of collector area since they depend only on the amount of exhaust energy from the turbine which is determined solely by the electric demand. The electric demand is always met, either through collector area augmentation or fossil fuel consumption.

Using the guideline that high-temperature solar energy is expensive and thus should not be dissipated during any period of the year, between 20,770 and 24,230 m^2 of north-south collectors or near 34,870 m^2 of east-west collectors are optimum to minimize fossile fuel consumption. As expected more east-west collectors are required to produce the same percentage solar input to the system.

---

* B. W. Marshall, "Analysis of a 1000-Home Solar Total Energy Community Using Clean Air Solar Intensity," SAND75-0097, Sandia Laboratories, May 1975.

TABLE VI

Comparison of Solar System Operation in a Community Total Energy Concept

Collector Area (m^2)	Storage Volume Storage 1 (m^3)	% Solar	Average Solar Energy Collected (J/Day x 10^{-11})	Average Fossil Fuel Consume J (J/Day x 10^{-11})		Average Energy Dissipated (J/Day x 10^{-11})	
				Furnace 1	Furnace 2	Tower 1	Tower 2
North-South Collectors							
0	0	0	0	6.1	1.66	0	0.19
5575	150	15	1.15	4.73	1.66	0	0.19
10385	250	30	2.14	3.48	1.66	0	0.19
13850	500	41	2.86	2.49	1.66	0	0.19
20770	1250	63	4.28	0.74	1.66	0	0.19
24230	1500	73	4.01	0.20	1.66	0.27	0.19
27700	1500	77	5.72	0.0	1.66	0.91	0.19
East-West Collectors							
17430	500	34	2.45	3.0	1.66	0	0.19
24400	1000	50	3.43	1.78	1.66	0	0.19
34870	1600	75	4.85	0.0	1.66	0.1	0.19

Economic analyses were performed using a computer program provided by Sandia's auditing department. In this analysis the levelized annual cost of energy over the expected lifetime of the system was calculated for each of the solar systems studied (see Task 2.2 for discussion of techniques). In addition, the costs were broken down to determine the major cost elements. Figure 27 presents these results and shows that fossil fuel, collectors, and thermal-distribution costs are the major components. In addition, the curve shows that a 65-% conservative energy system results in a levelized annual cost lower than the corresponding 100-% fossil fuel total energy system. In effect, collectors can be added to the system with lower costs than the anticipated fossil fuel costs up to the condition where overnight storage is provided. When the collector area is increased beyond this point, the cost increases as energy is wasted in the cooling towers and collector utilization is effectively lowered.

Because of the uncertainty in economic parameters, a range of conditions was selected and the levelized energy costs computed for each. These results are shown in Figure 28. Also shown on the zero-percent solar line are levelized annual costs for a normal home in Albuquerque not serviced by a total energy system but with loads identical to those calculated for the 1000-home community. Initial individual house energy costs were chosen as \$0.025/kWh for electricity and \$1.00/10^6 Btu for heating and hot water. Based on these results, minimum energy costs in the solar total energy system were from 40 to 60% more than those for a normal house.

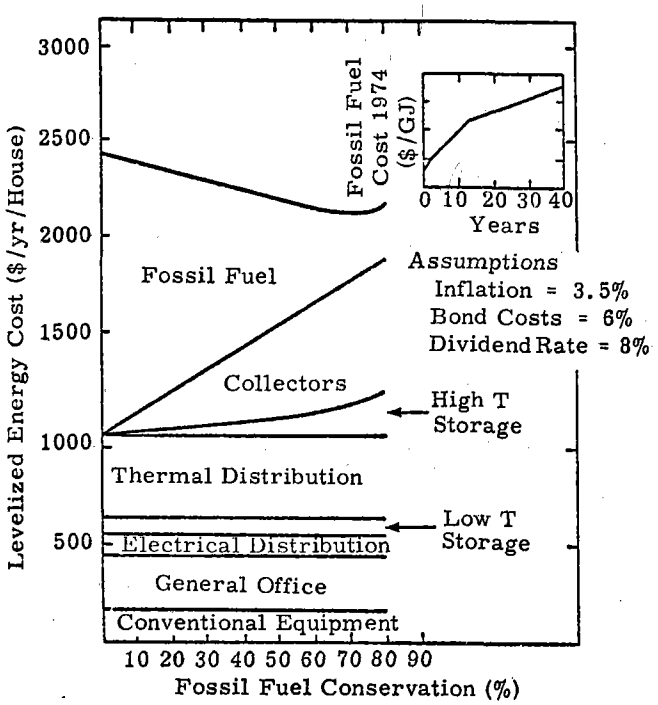

Figure 27. Solar Total Energy System Cost - 1000 Homes - Albuquerque, New Mexico (Assumes 30% conversion efficiency for electrical generation and 75% conversion efficiency for thermal requirements to compute fossil fuel needs of conventional system)

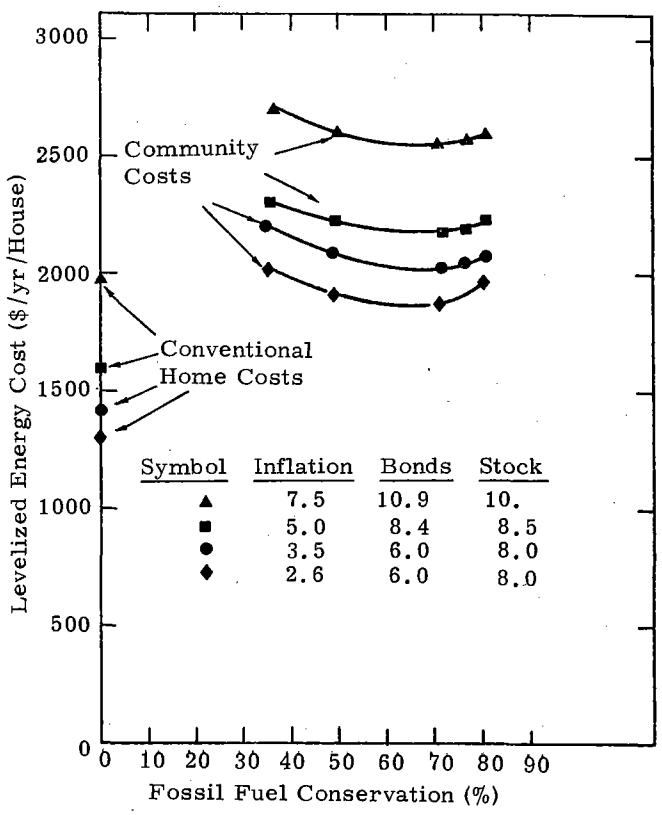

Figure 28. Annual Levelized Costs Comparison

With the availability of the 1962 Albuquerque solar and weather data (see Section 8.2), selected clear air intensity designs were reanalyzed to evaluate cloud effects. In particular the 63% solar system shown in Table VI with 20,770 m^2 of collector was used in the reevaluation. The collector output for a 6-day winter period is shown in Figure 29. Cloud effects during the last two days of the interval are apparent and similar periods were also observed in the data for the remaining three seasons.

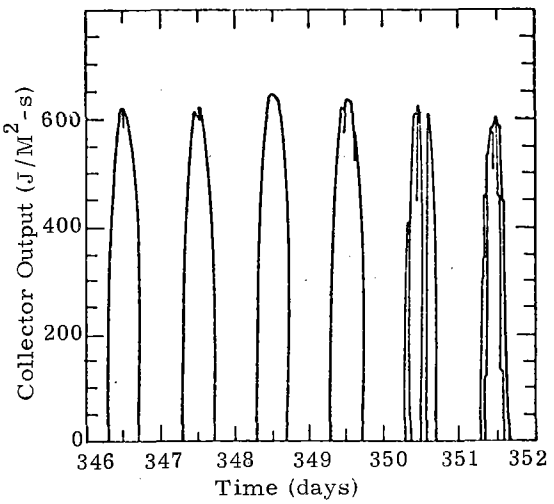

Figure 29. Collector Output for Winter Season

Modifications to the HLOAD subroutine for calculating thermal loads and improved estimates in the heat-transfer coefficients for individual homes were incorporated at this time and resulted in reduced thermal loads on the system. The revised loads are 8000 J/s (27,300 Btu/hr) peak and 3900 J/s (13,400 Btu/hr) average for the winter day. The corresponding loads in the previous analyses were 12,000 J/s (40,950 Btu/hr) peak and 6830 J/s (23,500 Btu/hr) average for the winter day. The response of the two storage systems is shown in Figure 30. The reduced insolation for days 350 and 351 is evidenced as a smaller increase in the volume of Storage 1 during the day.

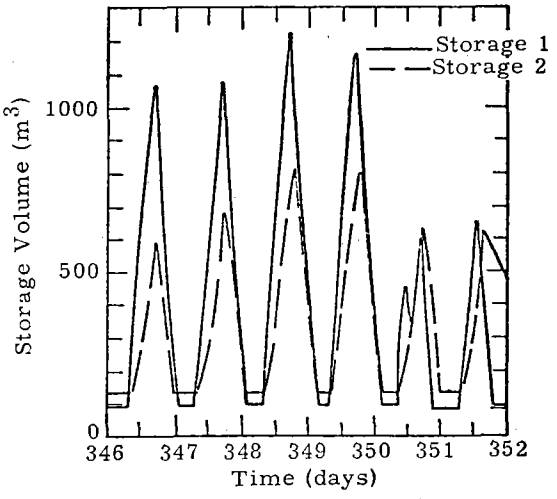

Figure 30. Response of Thermal Storage Systems for Winter Season

Assuming that the average of six days from each of the four seasons satisfactorily represents the average annual performance, one can estimate the percentage of the community energy needs supplied by solar energy. For a collector area of 20,770 m^2, 59% of the energy needs were supplied by solar input. For 24,330 m^2 of collector, 70% of the energy requirements are provided by solar input using the 1962 solar data. Because this analysis was performed during a period when load data were being modified, it is not possible to isolate the effect of using real day solar data. The reduced solar input and reduced thermal loads combine to cause little net effect on the relative contributions of solar and fossil fuel input compared to the results of the clear air solar insolation results.

Mixed-Load Community -- Future analyses will attempt to determine the breadth of application of the basic solar total energy concept. The mixed-load community described above will be employed to compute energy demands. In addition, subsets of the community will be used to provide load definitions. For example, the high-density load may be comprised of low- and high-rise apartments. Load profiles for military bases at various locations have been obtained from a study by R. L. Goen.*

Because of the flexibility designed into the SOLSYS mathematical model, a number of combinations of components may be assembled and evaluated, both technically and economically. Analyses of the systems outlined in Table VII have begun. In addition to the cascaded system using focusing collectors, use of flat-plate collectors will be studied in a noncascaded configuration. A system using focusing collectors for high-temperature energy and flat-plate collectors for low-temperature energy will be evaluated in both a cascaded and noncascaded configuration. In the cascaded system the flat-plate collectors are used to make up deficiencies in low-temperature energy. A total energy system which stores energy after conversion to electricity will also be evaluated. In this case the high-temperature storage will be eliminated, and thermal energy collected during the day will be immediately converted to electrical energy and stored in either a flywheel, battery system, or other electrical energy storage. Thermal energy not converted to electricity will be stored in a low-temperature thermal storage system. In addition, a concentrating collector configuration using photovoltaic cells located on the receiver tube will be examined. In this system, the receiver tube is maintained at a temperature high enough to produce useful thermal energy collection. Excess electrical energy from the photovoltaic system is stored in an electrical storage device such as a battery or flywheel for use at a different time of day.

These solar energy systems will be subjected to in-depth analysis for the same eight cities (Section 8.2) chosen to represent diverse climatological conditions. The utilities serving these cities have been contacted to obtain present and future fuel costs to use in economic comparison studies.

---

* Richard L. Goen, "Assessment of Total Energy Systems for the Department of Defense, Vol I," Stanford Research Institute, November 1973.

TABLE VII

Total Energy Systems Analysis

Analysis	High-Temperature* Collector	Electrical Storage	Cascaded	Low-Temperature* Make-up	Low-Temperature Storage	Load
1.	Parabolic Trough	Therminol-66†	Yes	None	Water	a. Mixed-Load Community
						b. High-Density Only
						c. Military Base
2.	Parabolic Trough	Therminol-66†	Yes	Flat-Plate	Water	a. Mixed-Load Community
3.	Parabolic Trough	Therminol-66†	No	Flat-Plate	Water	a. Mixed-Load Community
4.	Flat-Plate	Water	No	Flat-Plate	Water	a. Mixed-Load Community
5.	None	Battery	No	Photovoltaic/ Thermal	Water	a. Mixed-Load Community
						b. Single House
6.	Parabolic Trough	Flywheel	Yes	None	Water	a. Mixed-Load Community

* Backed up by fossil fuel

† High-temperature heat transfer fluid to drive turbine

Task 9. Phase IV-B Supportive Energy Research

9.1 Collector Fabrication Development

Alternate Trough Development -- The two polyester/fiberglass (2.7 x 3.7 m) troughs produced by the MFG Boat Company have been assembled in their mounting frames. The tracking and drive systems have also been assembled and tracking system evaluation is underway. Receiver tubes 3.7 m (12 ft) in length are in final stages of fabrication. Their completion will permit operation of these collectors with the existing test facility to determine their performance parameters.

Other Construction Methods -- Two of the twelve development parabolic shell sections (0.9 x 2.7 m) were fabricated as split sections with two concentric halves of 0.95 cm (0.375 in.) thickness vs a single shell 19 mm (0.75 in.) thick. These parabolic sections will be separated by 5 cm (2.0 in.) with a flexible honeycomb section bonded between the halves. The purpose of this approach is to determine the strength of such a structure to see if the rib and longitudinal framework underneath the trough may be eliminated. Development of a thin-shell honeycomb structure would significantly reduce the cost of materials, fabrication, and assembly.

In addition, a development contract has been placed with the Brunswick Corporation for fabrication of twelve parabolic trough sections 0.6 x 1.2 m (2 x 4 ft) on a precision metal mold.

Autoclave techniques will be used to investigate the effects of high pressure/temperature lamination of contoured parabolic shells on accurate metal tooling. One objective is to decrease the contour and slope errors of fabrication. Honeycomb sections will also be produced for structural evaluation.

Sagged Glass Mirrors -- Ten sagged glass sheets 6 x 160 cm (24 x 62.6 in.) and parabolic in contour have been silvered and coated with protective paint. Six of these sheets will be applied to cover half the surface of a prototype 2.7 x 3.7 m collector unit now being assembled. This unit will be tested in the collector test facility fluid loop to determine its system operational parameters. The outdoor installation will subject it to typical environmental conditions. Specular reflectance of these mirrors has been measured as 0.84 to 0.88 on flat samples of the same glass silvered by the same process.

Reflector Material Evaluation -- Specular solar reflectance properties of a variety of aluminized and silvered materials have been obtained, and the initial results for the most promising candidates are listed in Table VIII. For the specular measurements the samples were mounted on an optically flat specimen holder, and therefore the results represent the solar reflectance properties under ideal conditions. Although data were obtained from 0.13° (full width, half height) to 1.0°, only solar reflectance at the 1.0° aperture is reported here. The values in the table indicate that silvered materials have better solar reflectance properties than aluminized materials, and that all of the materials listed have better specular reflectance than Alcoa's Alzak. However, it should be pointed out that in bonding metallized film to a secondary surface, a so-called "orange peel" texture (caused most likely by the adhesive system used, but also by dust particles, film tension, shrinkage, etc.) can reduce the specular reflectance by more than 20%.

Samples of all of these materials are being subjected to both outdoor and accelerated environmental testing with periodic specular reflectance measurements. Three Sheldahl reflector materials (two aluminized and one silvered) are being procured for use on the 18.3-m troughs. In addition, the 3M Company is studying alternate adhesive systems to eliminate a severe "orange peel" problem associated with their decorative product Scotchcal®. At the present time, Alzak remains a backup reflector.

TABLE VIII

Solar Reflector Materials

Manufacturer	Product	Material	Reflective Surface	Specular Solar Reflectance RS (1°)	Hemispherical Solar Reflectance Rs (2Π)
Sheldahl	G400300	2 mil Teflon silver-Inconel	2nd	0.89	0.98
Sheldahl	G401500	5 mil Teflon silver-Inconel	2nd	0.87	0.98
Sheldahl	- ①	2 mil Mylar silver-Inconel	1st③	0.89②	0.95②
Sandia	Curved glass	ASG sheet silver	2nd	0.84 to 0.88	0.90
3M Co.	Scotchcal 5400	2 mil acrylic aluminum	2nd	0.85	0.89
Sheldahl	G405600	2 mil Teflon aluminum plus 2 mil Mylar	2nd	0.80	0.87
Sheldahl	-①	2 mil Mylar aluminum	1st③	0.80②	0.89②
3M Co.	Sprint 530	2 mil Mylar aluminum	2nd	0.75	0.84
Alcoa	Alzak Type M1	Electropolished aluminum lighting sheet	1st③	0.71	0.83

① Ordered for 18.3-m (60-ft) troughs
② Sheldahl data
③ First surface reflector has protective coating

9.2 Storage Technology

Although the Solar Total Energy Test Facility is currently committed to sensible heat storage, other techniques are being considered. The high-performance flywheel looks interesting and feasible because kinetic energy is high quality and can be converted to electricity with good efficiency. The amount of stored energy required is smaller than the equivalent sensible heat energy storage; the latter must pass through the relatively inefficient thermodynamic cycle to produce electricity. A proposal to build a flywheel energy system for the solar project has been presented to ERDA Conservation Division and EPRI. Development would rely heavily on the expertise of private industry, with Sandia Laboratories doing the system integration and industry providing the subsystems.

9.3 Theoretical Studies

Energy Deposition on the Absorber Tube -- A preliminary version of a refined computer program for analyzing solar collectors has been written. It computes the energy absorbed by the

absorber tube, as a function of position, in a solar collector whose reflector is a parabolic trough. Statistical methods are used to approximate the effects of imperfections in the construction and the operation of the collector. Optical properties of the various system components are also included in the computation. The output of this program is used as input to heat-transfer calculations needed to analyze the overall performance of the solar collector.

In practice, several effects combine to cause departure from ideal behavior:

- The incoming sunlight is not perfectly collimated.
- There are aiming errors in the tracking system.
- There are slope errors and other imperfections in the reflecting surface; these errors may be a function of position on the reflector.
- The absorber tube is not accurately positioned on the focal line; this error may be a function of position along the tube.

All of these effects are treated by considering the reflected light to have a distribution of directions described by a probability density.

Figure 31 examines S, the power absorbed per radian by a unit length of the receiver tube, as a function of β, the angular distance along the receiver tube from the axis of the parabola. The value S is shown divided by the product of the focal length (f) and the solar insolation (a_o) to provide convenient dimensionless plotting parameters. The curves are parameterized in $\sigma/(r/f)$ where σ indicates the amount of dispersion of the solar beam upon reflection from the reflector and r is the receiver tube radius. Ideal reflection, no dispersion, and neglecting the solar disc size implies that $\sigma = 0$ and that the distribution function representing the dispersion of the solar beam is in fact a delta function. The computations were performed assuming monochromatic radiation, a collector tilt angle of 0°, a rim angle of 90°, an absorber tube radius of 2.06 cm (0.812 in.), and a mean radius of 3.29 cm (1.295 in.) for the glass envelope. The receiver tube is assumed to be exactly at the focal line of the parabolic trough. Curves A, B, and C include the following additional assumptions.

Trough reflectance = 1.0
Glass envelope transmittance = 1.0
Receiver tube absorbance = 1.0.

Curve A shows a drop to zero at 2.7° which is due to shadowing at small angles and an additional drop to zero at 90° because the incident light misses the parabola at larger angles. Thus, for the ideal case, most of the solar energy is absorbed by the receiver tube near 90°. Curves B and C show the effect of increased beam dispersion on the ideal distribution. Curve D is for the more realistic situation in which the glass envelope transmittance and receiver tube absorptance were obtained from Figure 32.

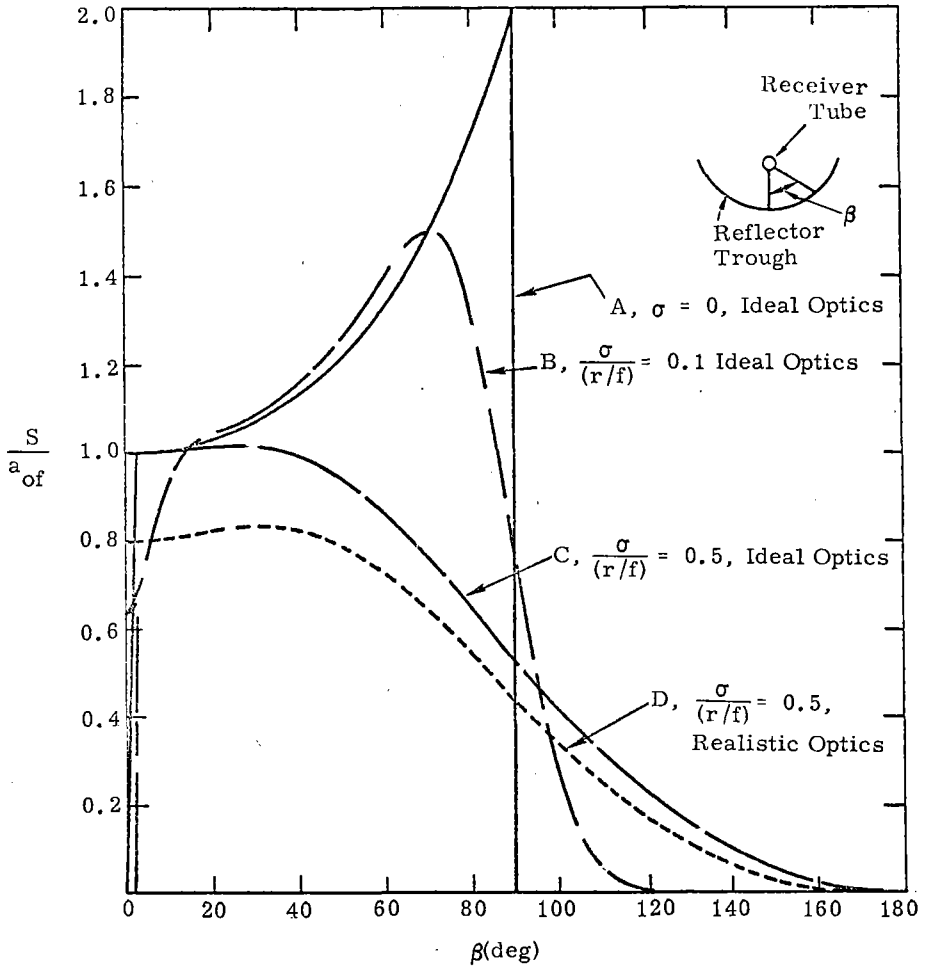

Figure 31. Power Absorbed by Receiver Tube Versus Angle β for Values of Standard Deviation

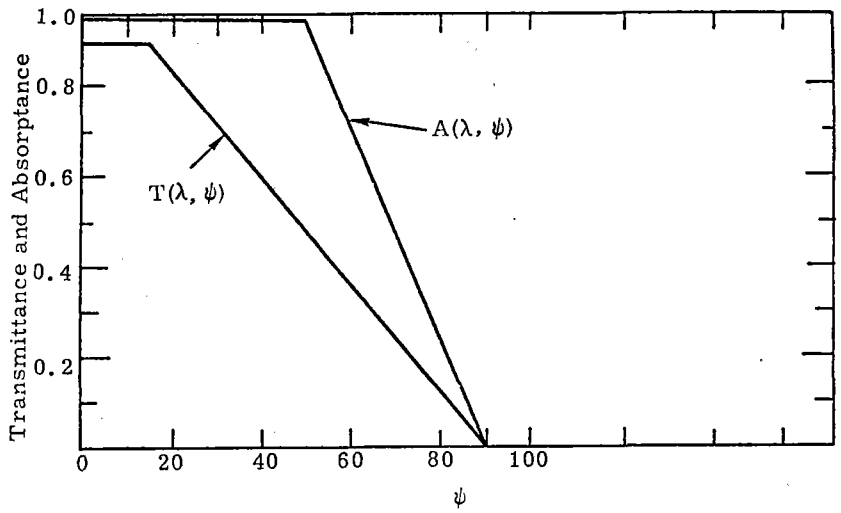

Figure 32. Approximate Transmittance T of the Glass Envelope and Absorptance A of the Absorber Tube as a Function of Incident Angle ψ

The present version of the computer program uses a monochromatic spectrum (or some average spectrum) and either the ideal optics or the data presented in Figure 32. The program requires about 43,000 words of central memory and runs in about three seconds on the CDC 6600 to provide solutions such as those shown in Figure 31.

Planned future work on this program includes the following:

- Provide better data for collector reflectance, transmittance, and absorbance.
- Calculate energy deposited in the envelope as a function of β and length down the tube receiver including end effects.
- Use nonmonochromatic light.
- Polarization effects -- Although the incoming sunlight may be unpolarized, this can change upon reflection from the reflector. The subsequent optics for transmission through the envelope and absorption on the absorber tube may depend on polarization. The computer program can be changed to include these effects.
- Thick envelope calculation -- The present program uses the assumption that the envelope is thin in comparison with the absorber-tube radius. The computation can be modified to apply to a thick envelope.
- Use a more general probability density function than the one used in the present program if detailed knowledge of this distribution becomes available and indicates that a normal distribution is not adequate.
- Insulating strip considerations -- Put in an option to include direct sunlight on the back of the absorber tube.

A report describing the computer program and its capabilities in detail will be written.

Task 10. Coating Evaluation

The goals for a selective receiver tube coating include the requirement for an inexpensive process yielding a coating with absorptance and emittance as follows: $\alpha_s \geq 0.95$, $\epsilon_{315°C} \leq 0.3$. A survey of candidate coatings has been conducted.* A summary of some of the coatings surveyed is presented in Table IX.

*D. M. Mattox, "Applications of Thin Films to Solar Energy Utilization," SAND75-0263, Sandia Laboratories, to be published.

TABLE IX

Properties of Selective Solar Absorber Coatings

Material	Fabrication Technique	α_s	$\epsilon_{H,T}$(Low T)	$\epsilon_{H,T}$(High T)	Stability °C
Gold	Gas Evaporation	>0.99	<0.1	---	<100
Germanium	Gas Evaporation	0.91 [0.98]	0.2 (160) [0.5(250)]	0.5(350)	
	Vacuum Evaporation	0.61	0.54(240)		
	Paint (silicone binder)	0.91	0.8 (200)		
Silicon	CVD (+AR coating)	0.75		0.08(500)	<500
	Vacuum Evaporation				
	Paint	0.83	0.7(200)		
Be + 1% Cu	Anodized	0.91 [0.84]		[0.3(550)]	
Aluminum	Anodized (organic dye)	0.96		0.98(350)	<350
	Anodized (K MnO_4 dye)	0.80	0.35(<100)		
PbS	Vacuum Deposited	0.98	0.2(240)	0.3(300)	>300
	Paint (silicon binder)	0.94	0.8(200)		
Cu_2S	Chemical Conversion	0.79	0.2(200		
NIS - ZnS	Electrodeposited - 1 Layer	0.88	0.1(100)	0.16(300)	<220
	2 Layer	0.96	0.07(100)		<280
WC + Co	Plasma Spray	0.95 (600)	0.28(200)	0.4(600)	>800
Cr_xO_y	Paint (silicone binder)	0.98	0.92(200)	0.9(900)	>900
	Electrodeposited	0.95	0.1(100)	0.2(350)	
+ Co	Plasma Spray	0.90 (800)		0.5(800)	>800
CuO - Cu_2O	Chemical Conversion	0.91	0.16(<100)	0.4(200)	<200
	Chemical Spray	0.93	0.11(80)		
Co_3O_4	Thermal Oxide	0.90	0.3(140)		>1000
304 Stainless Steel	Chemical Conversion	0.91			
	Thermal Oxide (760°C)	0.82	0.15(100)	0.2(300)	
Steel (Fe_3O_4)	Chemical Conversion	0.90	0.07(90)	0.35(200)	
MULTILAYER FILMS					
Al_2o_3 - Mo - Al_2O_3	Vacuum Evaporation	0 0.85 [0.97]	[0.34(100)]	0.11(500); [0.4(350)]	<900
SiO - Cr - SiO	Vacuum Evaporation	0.88	<0.1		<450
MgF_2 - Sn (Part.)	Vacuum Evaporation	>0.95	0.1		

Note: Numbers in parenthesis are temperatures, °C, at which measurements were made.
ϵ values in brackets correspond to α values in brackets.

Studies on electrodeposited black chromium have shown that improved solar absorptance ($\alpha_s = 0.95$) and low total hemispherical emittance ($\epsilon_{300°C} = 0.21$)† can be obtained by increasing substrate roughness over that normally obtained with bright nickel. Increasing surface roughness can result in improved α_s as a function of angle of incidence. Some of these data are shown in Figures 33; surface roughness increases from curve 1 to curve 3 in Figure 33(a).

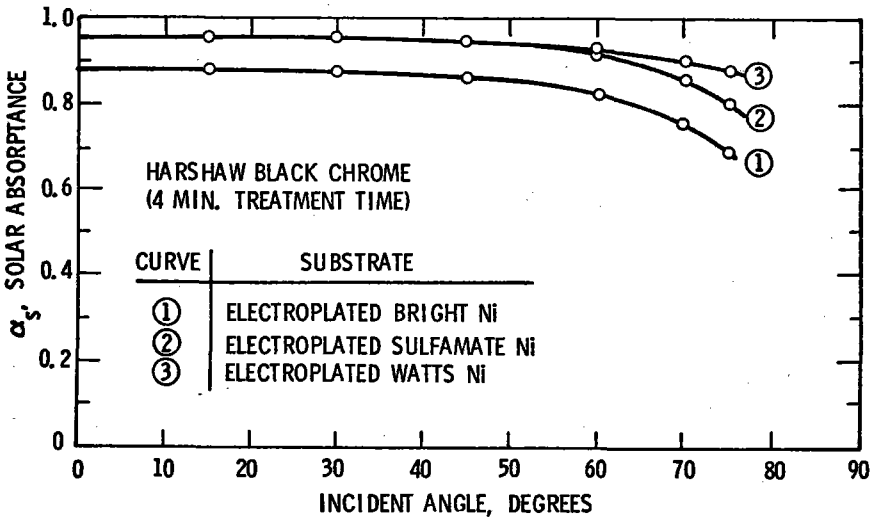

(a)

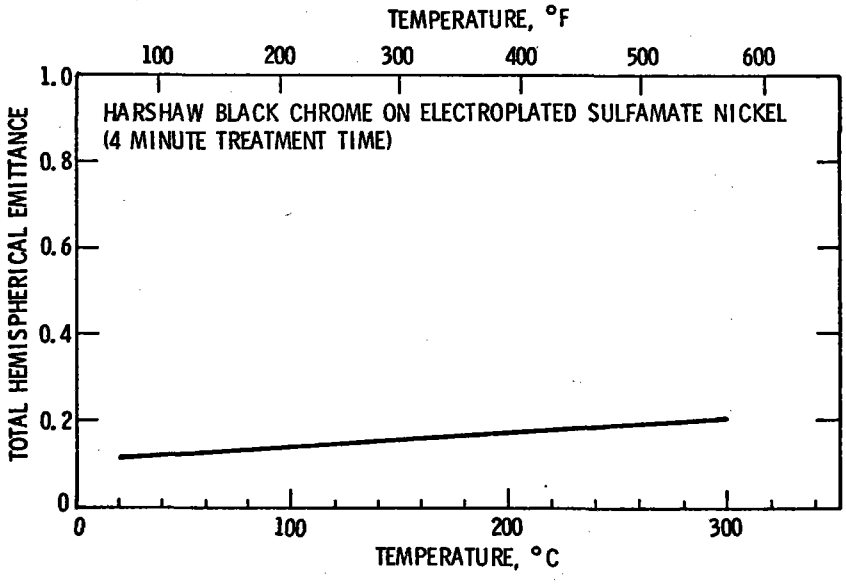

(b)

Figure 33. Effect of Substrate on Selective Black Chrome

†The emittance measurement equipment will be described in SAND75-0079, "Total Hemispherical Emittance Measurement Apparatus for Solar Selective Coating Applications," R. B. Pettit, Sandia Laboratories, to be published.

The best results have been obtained by black chrome plating over thick 0.025 mm (0.001-in.) sulfamate nickel on bead-blasted steel. Close control must be maintained in all plating processes to obtain optimum properties.

The thickness of the black chrome is in the range of 1500 to 2000 Å. The composition varies through the coating. At the nickel/black-chrome interface a region of almost pure metallic chromium is deposited. Approaching the outer surface, the chromium-to-oxygen ratio is about 1:1. Evidence indicates that in this region the coating consists of fine chromium particles suspended in a Cr_2O_3 matrix.

In essence, the black chrome absorbs the solar energy and the sulfamate nickel acts as the predominant infrared emitting surface. The emittance of Sulfamate nickel on steel is about 0.12 at 300°C.

Task 11. Technology Utilization

The Sandia Solar Total Energy Program has advanced to the point that a Solar Total Energy Technology Symposium has been planned. The symposium will be at Sandia Laboratories and is tentatively scheduled for July 1975. Preliminary arrangements for speakers and colloquium topics are underway.

The reports and presentations listed in Section II represent the major vehicles for information dispersement during this reporting period.

SECTION IV. APPENDICES

A. Solar Total Energy System Costs

The determination of cost competitiveness of solar energy systems is subject to wide fluctuations depending on the assumptions made concerning such things as collector and future fuel costs. Thus, the assumptions employed in the cost analysis presented in Task 2.2 are outlined in detail for a solar total energy system requiring 24,376 m^2 of parabolic trough collectors which conserves, on the average, 76% of the total fossil fuel requirements of an array of 1000 separated homes. All costs are in 1974 dollars.

I. Power Generation Plant

A. Initial Investments

- Land and land projects - $34,000

  34 acres at $1000/acre, to locate collectors and power plant equipment.

- Structures and improvements - $80,000

  Buildings to house equipment, control rooms, maintenance equipment, etc.

- Conventional equipment - $710,000

  2.2-MW turbogenerator system complete with all required support equipment.

- Solar equipment - $4,650,000

Collectors at $107.60/$m^2$	$2,620,000
High-temperature storage at $4.75/MJ	1,290,000
Low-temperature storage at $1.9/MJ	480,000
Piping and controls	260,000

B. Future Costs

- Salvage Value - $150,000

  Approximately 3% of the power generation plant costs

- Major Overhaul and Replacement

  Overhaul - $10,000 to $20,000 every 4 years for the turbine system.

  Replacement of solar equipment - $110,000 each time is assumed at 8, 20, and 28 years.

- Operating Cost - $40,000

  Based on extrapolation of data for larger units.

- Maintenance Cost - $15,000

  Based on $.001/kWh for maintenance other than overhaul, fuel, operating labor.

- Fuel Cost - $29,600

  Based on average annual fuel consumption and an initial energy cost of $0.43/GJ.

II. Transmission Plant

No costs were included here as it is assumed that the power plant is near the community.

III. Distribution Plant No. 1 - Electrical Distribution System

A. Initial Investment

- Land and land rights - $30,000

  $1,000/acre for purchase of land to locate buildings and purchase of rights of way where necessary.

- Structures and improvements - $40,000

  For structures necessary to house equipment, maintenance supplies, trucks, etc.

- Equipment - $200,000

  For construction of distribution system throughout community, based on estimate from utility company for 1000-home community.

B. Future Costs

- Salvage value and major replacement - $0

- Operating Cost - $25,000

  Based on estimates from utility companies for operation of a system this size.

- Maintenance Costs - $10,000

  Estimate based on utility company recommendations.

IV. Distribution Plant No. 2 - Thermal Distribution System

A. Initial Investment

- Land and land rights - $10,000

  For land to locate plant with pumps and other equipment.

- Structures and improvements - $60,000

  Structures to house equipment for system.

- Equipment - $2,250,000

  Estimated cost of all piping, pumps, controls, gages, etc. to provide entire 1000-home system.

B. Future Costs

- Salvage value - $100,000

  Approximately 4% of equipment costs.

- Major replacement costs - $225,000

  At 15 years 10% of system first cost to provide major overhaul.

- Operating cost - $40,000

  Estimate of personnel to provide system operation

V. General Plant

A. Initial Investment

- Working capital - $150,000

  Capital necessary to begin operation of utility service.

- Land and land rights - $10,000

  For land to locate general plant.

- Structures and improvements - $100,000

  For building-to-house general manager, accounting and public relations types, records, accounts, etc.

- Furniture and equipment - $25,000

  Furniture for offices

B. Future Costs

- Salvage value - $50,000

- Major replacement - $50,000

  At 15 years for major renovation of plant

- Operating cost - $80,000

  Salaries of general manager, billing and accounting staff, etc.

- Maintenance cost - $15,000

  Estimate of maintenance of buildings and offices.

VI. Miscellaneous Data

This section is composed of the various economic factors including inflation, bond interest rate, expected lifetime, expected fuel increase rate, and other factors. Typical values used in these analyses were as follows

Inflation rate	3.5%
Bond interest rate	6 %
Stocks interest rate	8 %
% in stocks	40 %
Fixed charge rate (for taxes, etc.)	2.6%
Expected lifetime	30 years
Fuel increase rate No. 1	45 %
Years	1974-1975
Fuel increase rate No. 2	11.5%
Years	1976-1985
Fuel increase rate No. 3	1.5%
years	1986-2004

These data provide the basis for the economic analyses reported in Task 2.2. Other solar collector areas result in different total collector costs, storage costs, and fossil

fuel costs. However, the unit costs of each of these remain the same as that reported here. Distribution system costs, both electrical and thermal, and general plant remain constant for all values of collector area.

B. Program Technical Contributors*

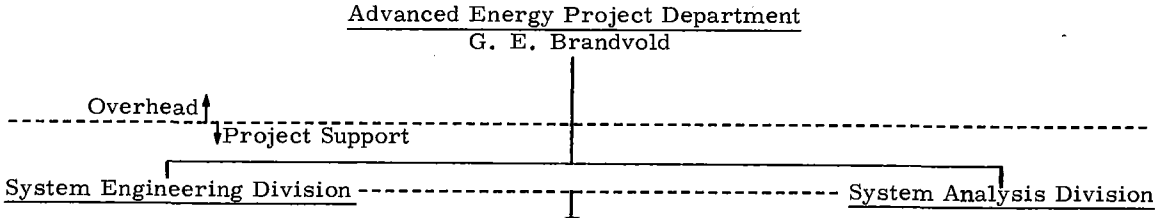

System Engineering Division

R. H. Braasch

System Engineers
- J. D. Cyrus
- J. A. Leonard
- B. J. Petterson
- S. Thunborg
- A. F. Veneruso

Component Designers
- R. L. Champion
- G. W. Treadwell
- L. E. Torkelson

Technicians
- L. N. Ernst
- G. L. McCoach
- R. S. Rusk

Program Support

Thermal Analysis
- W. H. McCulloch
- M. E. Fewell
- J. P. Abbin

Data Processing
- W. W. Shurtleff
- M. S. Hill
- T. E. Smart
- E. D. Young

Storage Technology
- R. A. Milby

Air Conditioning Design and Control
- A. V. Farnsworth

Structural Analysis and Design
- P. P. Stirbis
- G. W. Hughes

Plant Engineering
- E. E. Rush
- C. K. Rudy

Theoretical Analysis
- F. Biggs

Material Evaluation and Testing
- T. P. Conlon
- L. G. Rainhart
- R. G. Pettit
- D. M. Mattox
- G. J. Kominiak
- R. R. Sowell
- B. L. Butler
- R. L. Lachance
- E. K. Beauchamp
- K. T. Gillen
- T. M. Meyers
- D. W. Tipping
- J. M. Freese
- G. D. Miller
- O. W. Miller

Instrumentation and Control
- T. C. Sheives

System Analysis Division

R. P. Stromberg
- G. V. Barton
- M. W. Edenburn
- R. W. Harrigan
- B. W. Marshall
- D. E. Randall
- E. C. Boes

*This list includes part-time contributors.

DISTRIBUTION

George McKoy
Manager, Solar Projects
Energy Projects Group
P. O. Box 92957
Aerospace Corporation
Los Angeles, CA 90045

Peter Susey
American Gas Association
1515 Wilson Boulevard
Arlington, VA 22209

Solomon Zwerdling
Director of Solar Energy Programs
Argonne National Laboratory
Bldg. 362-C181
9700 South Cass Ave.
Argonne, IL 60439

Leonard S. Raymond
University of Arizona
Optical Sciences Center
Tucson, AZ 85721

Barber-Nichols Engineering
6325 West 55th Ave.
Arvada, CO 80002

F. M. Smits
Bell Laboratories
555 Union Boulevard
Allentown, PA 18103

Solar Energy Application Laboratory
Colorado State University
Ft. Collins, CO 80521

Harold Bullis
Science Policy Division
Congressional Research Service
Library of Congress
Washington, D.C. 20540

Karl W. Boer
Institute of Energy Conversion
University of Delaware
Newark, DE 19711

Louis O. Elsaesser
Director of Research
Edison Electric Institute
90 Park Avenue
New York, NY 10016

Energy Research and Development
Administration (40)
1800 G Street, N.W.
Washington, D.C. 20550
Attn: George Kaplan (20)
James E. Rannels (20)

Energy Research and Development
Administration
Division of Military Application
Washington, D.C. 20545
Attn: Major Gen. Frank A. Camm

Energy Research and Development Administration (2)
Division of Applied Technology
Germantown, MD 20767
Attn: Edward H. Fleming (1)
Lou B. Werner (1)

Energy Research and Development Administration (4)
Albuquerque Operations Office
Albuquerque, NM 87115
Attn: J. R. Cotton (1)
D. K. Nowlin (1)
J. W. Schroer (1)
R. W. Scott (1)

Dwain Spencer (5)
Electric Power Research Institute
3412 Hillview Ave.
Palo Alto, CA 94304

J. E. Guthrie
Envirodynamics, Inc.
3700 McKinney Ave.
Dallas, TX 75204

Federal Energy Administration (2)
1200 Pennsylvania Ave., N.W.
Washington, D.C. 20461
Attn: Samuel J. Taylor (1)
Frank Zarb (1)

Richard Hill
Federal Power Commission
441 G Street, N.W., Room 4005
Washington, D.C. 20426

R. Schmidt
Systems & Research Center
Honeywell Incorporated
2700 Ridgeway Road
Minneapolis, MN 55413

Alan R. Siegel, Director
Environmental Factors & Public Utilities Division
Department of Housing & Urban Development
Washington, D.C. 20410

Lorin L. Vant-Hull
Department of Physics
University of Houston
3801 Cullen Boulevard
Houston, TX 77004

H. Silha
University of Idaho
Moscow, ID 83843

Martin Prochnik
Deputy to the Science Advisor
U. S. Department of Interior
Room 5204
Washington, D.C. 20204

G. C. Szego, President
Intertechnology Corporation
Box 340
Warrenton, VA 22186

DISTRIBUTION (cont)

Michael Wahlig
Lawrence Berkeley Laboratory
Building 50A, Room 6121
University of California
Berkeley, CA 94720

L. Hunt Sutherland
Lone Star Gas Company
901 S. Harwood St.
Dallas, TX 75201

Los Alamos Scientific Laboratory (2)
Los Alamos, NM 87544
Attn: J. D. Balcomb, 571 (1)
H. P. Deinken, ADWP-1 (1)

Floyd Blake
Martin Marietta Aerospace
Denver Division
P. O. Box 179
Denver, CO 80201

Jerry O. Bradley
Midwest Research Institute
425 Volker Boulevard
Kansas City, MO 64110

O. N. Salmon
Advance Research Programs Laboratory
Central Research Laboratory
3M Center
St. Paul, MN 55101

C. Peyton
Specialty Products Business Group
Monsanto Company
800 N. Lindbergh Boulevard
St. Louis, MO 63166

Karl Willenbrock, Director
Institute for Applied Technology
National Bureau of Standards
Room B-112 - Tech (400.00)
Washington, D.C. 20234

R. L. San Martin
New Mexico State University
Las Cruces, NM 88001

W. A. Cross
Attn: M. W. Wilden
Department of Mechanical Engineering
University of New Mexico
Albuquerque, NM 87113

C. Faulders, SK90
North American Rockwell
Space Division
12214 Lakewood Boulevard
Downey, CA 90241

John M. De la Castro
Northern Natural Gas Co.
2223 Dodge St.
Omaha, NB 68102

M. W. Rosenthal
Oak Ridge National Laboratory
P.O. Box Y
Oak Ridge, TN 37830

Richard Balzhizer
Office of Science & Technology
Executive Office of the President
Washington, D.C. 20506

Ronal Larsen
Office of Technology Assessment
Old Immigration Building, Rm 722
119 D Street, NE
Washington, D.C. 20002

A. R. Spangler
Omaha Public Power District
1623 Harney
Omaha, NB 68102

Jesse C. Denton
National Center for Energy Management and Power
University of Pennsylvania
113 Towne Building
Philadelphia, PA 19104

Public Service Company of New Mexico (2)
P. O. Box 2267
Albuquerque, NM 87103
Attn: Edward Kist (1)
G. Schreiber (1)

Gus Dorough
Deputy Director for Research and
Advanced Technology
The Pentagon, Room 3E114
Mail Stop 103
Washington, D.C. 20540

Ross Stickley
G.T.S. Sheldahl Company
Northfield, MN 55057

Roland Kurth
Solar International
300 Wyoming, N.E.
Albuquerque, NM 87112

Ira Thierer
Southern California Edison
P. O. Box 800
2244 Walnut Grove Avenue
Rosemead, CA 91770

S. Cunningham
Southern California Gas Co.
P. O. Box 3249
Terminal Annex
Los Angeles, CA 90051

J. O. Carnes
Southern Union Gas Company
Fidelity Union Tower Building
Room 1537
1507 Pacific Avenue
Dallas, TX 75201

DISTRIBUTION (cont)

B. D. Daugherty
Southern Union Gas Company
723 Silver SW
Albuquerque, NM 87103

A. Warren Adam
Sundstrand Electric Power
4747 Harrison Avenue
Rockford, IL 61101

Carroll V. Kroeger, Sr.
Director, Tennessee Energy Office
Suite 250
Capitol Hill Bldg.
Nashville, TN 37219

Jack A. Harris
Marketing Services Manager
Texas Electric Service Co.
P.O. Box 970
Fort Worth, TX 76101

Commanding General
White Sands Missile Range, NM 88002
Attn: STEWS-TE-NT
Marvin Squires

1100 C. D. Broyles, Attn: 1110 J. D. Kennedy
1120 G. E. Hansche
1540 T. B. Lane, Attn: 1543 H. C. Hardee
2300 L. D. Smith
2320 K. Gillespie, Attn: 2324 L. W. Schulz
2400 R. S. Claassen
2440 O. M. Stuetzer, Attn: 2441 G. W. Gobeli
4700 D. B. Shuster
4730 A. A. Lieber Attn: 4734 V. L. Dugan
5000 A. Narath, Attn: 5100 J. K. Galt
5600 A. Y. Pope
5110 F. L. Vook
5130 G. A. Samara
5150 J. E. Schirber
5200 E. H. Beckner
5220 J. V. Walker, Attn: 5223 J. H. Renken
5620 R. C. Maydew
5700 J. H. Scott, Attn: 5720 M. L. Kramm
5710 G. E. Brandvold, Attn: 5716 W. N. Caudle
5712 R. H. Braasch (100)
5717 R. P. Stromberg (50)
5718 M. M. Newsom
5800 L. M. Berry, Attn: 5820 R. L. Schwoebel
5830 M. J. Davis, Attn: 5834 D. M. Mattox
5840 D. M. Schuster, Attn: 5842 R. C. Heckman
5846 E. K. Beauchamp
8100 L. Gutierrez
8180 C. S. Selvage, Attn: 8184 A. C. Skinrood
9300 L. A. Hopkins
9330 A. J. Clark, Jr. Attn: 9331 P. H. Adams
9340 W. E. Caldes, Attn: 9344 J. L. Mortley
9400 H. E. Lenander
9410 R. L. Brin, Attn: 9412 R. K. Petersen
9700 R. E. Hopper, Attn: 9740 H. H. Pastorius
9750 R. W. Hunnicutt

6011 G. C. Newlin
3141 L. S. Ostrander (5)
8266 E. A. Aas (2)
3151 W. L. Garner (3)
for ERDA/TIC (unlimited release)
3171-1 R. P. Campbell (500)
for ERDA/TIC - UC-62

Org.	Bldg.	Name	Rec'd by*	Org.	Bldg.	Name	Rec'd by*

*Recipient must initial on classified documents.